OBSERVATIONS ON THE LIFETIMES OF THE 3.37-Mev 2^+ STATE OF Be^{10} AND OF THE 6.14-Mev 3^- STATE OF O^{16}

Thesis by

Donald Kohler

In Partial Fulfillment of the Requirements

For the Degree of

Doctor of Philosophy

California Institute of Technology

Pasadena, California

1959

ACKNOWLEDGMENTS

The author gratefully acknowledges the assistance and encouragement offered him by all of the personnel of the Kellogg Radiation Laboratory. He is particularly indebted to Professors C. A. Barnes, R. F. Christy, W. A. Fowler, and T. Lauritsen for their help and advice.

Further, it is a special pleasure for the author to acknowledge his great indebtedness to Henry H. Hilton with whom the work on O^{16} was carried out.

Finally the author would like to express his appreciation for the support given this research by the joint program of the Office of Naval Research and the U. S. Atomic Energy Commission.

TABLE OF CONTENTS

TABLE OF CONTENTS Cont.

ABSTRACT

An upper limit for the lifetime of the 3.37-Mev 2^+ state of Be^{10} has been established by use of a Doppler shift technique. Be^{10} nuclei were produced by the Be^9 (d,p)Be^{10} reaction and those protons leaving the Be^{10} in its 3.37-Mev excited state were used to select γ rays emitted by Be^{10*} nuclei having a well defined recoil velocity. The energy of the γ rays emitted by these nuclei was determined by scintillation spectroscopy. The experiment was designed to look for a possible difference between the γ-ray Doppler shifts produced when the recoil nuclei were stopped in a metal foil and when the nuclei were allowed to recoil into vacuum. A small statistically insignificant difference in shift was observed which allowed only an upper limit of about 2.0×10^{-13} seconds for the half-life [mean life: $\tau \lesssim 3.0 \times 10^{-13}$ seconds] to be inferred. This limit to the mean life is compared with theoretical estimates of the lifetime based on different nuclear models.

The lifetime of the 6.14-Mev 3^- state of O^{16} has been measured by means of a recoil technique. The spatial distribution of decays of recoiling O^{16} nuclei, produced by the $F^{19}(p, \alpha_1)\ O^{16*}$ reaction, was studied with a highly collimated γ-ray detector. Comparison with the corresponding results obtained when the O^{16} nuclei were stopped at the target surface by an evaporated metallic layer provided a convenient means of determining the lifetime. A value for this half-life of $(8.6 \pm 4.0) \times 10^{-12}$ seconds [mean life: $\tau = (1.2 \pm 0.6) \times 10^{-12}$ seconds] has been found, consistent with previously established limits. The measured value of the mean life is compared with the theoretical values of the lifetime according to various nuclear models.

I. INTRODUCTION

One of the most powerful approaches to the problem of determining the properties of nuclear wave functions is to be found in the study of the interaction of nuclei with the electromagnetic field. Because an essentially complete and exact theory of the electromagnetic field and its interaction with charges and currents already exists one can, in principle at least, use experimental information on these interactions to obtain unambiguous and very useful knowledge of the nuclear wave functions. It is primarily for this reason that a determination of γ-ray lifetimes can be of significance to the problem of improving the understanding of the nature of the atomic nucleus, and eventually perhaps, also the nature of the nuclear forces themselves.

A number of experimental techniques have been developed for the measurement of γ-ray partial lifetimes or the corresponding γ-ray partial widths. These various methods differ widely in detail and their usefulness depends critically on the order of magnitude of the lifetime involved.

In the realm of very long lifetimes, i.e. long compared to the time normally available for observation of the decay, one would have to determine the lifetime from a measurement of the specific activity of the decaying nuclei. For somewhat shorter lifetimes one can actually follow the decay of the gamma-emitting activity and obtain directly from this the corresponding lifetime. This latter technique can, with the help of appropriate electronic instrumentation, enable one to measure lifetimes down to the order

of a few times 10^{-9} seconds. Delayed coincidence schemes, which allow one to "follow" the decay of a single excited nucleus rather than that of a statistical ensemble of such nuclei, allow the measurement of lifetimes in the range from perhaps 10^{-4} seconds down to about 10^{-11} seconds under especially favorable circumstances. Recoil techniques utilize the motion of the nucleus produced in a nuclear reaction creating the excited state to give a spatial distribution of decays which is then studied by an appropriately collimated γ-ray detector. This technique can be used in the range from about 10^{-6} seconds down to a few times 10^{-12} seconds under favorable circumstances. Doppler shift techniques require a knowledge of the slowing-down times of recoiling nuclei in different materials and accurate measurements of the attendant shift in the γ-ray energy. This method can be useful for measuring lifetimes in the range from about 10^{-11} seconds to a few times 10^{-15} seconds for solid stopping materials and of course for lifetimes of considerably longer-lived states if gaseous stopping materials are used. Resonance scattering of γ rays through an excited nuclear state provides a means of measuring partial γ-ray lifetimes for ground state transitions in the available nuclear species. Partial γ-ray lifetimes shorter than about 10^{-12} seconds may be measured by this method. Coulomb excitation also provides a method for indirectly measuring partial lifetimes for ground state transitions. Under favorable circumstances states with lifetimes up to 10^{-7} seconds have been measured this way. Finally for γ rays which compete with one or more particle reactions, i.e. for those from unbound nuclear states, one may

determine the γ—ray partial lifetimes from a measurement of the γ—ray and particle production cross sections. The useful range of this last method is limited only by the γ—ray detection sensitivity achieved in the cross section measurements.

The two experiments on Be^{10} and O^{16} to be described in the following were applications of the Doppler shift technique and recoil technique respectively.

No previous attempt to measure the lifetime of the 3.37-Mev 2^+ state of Be^{10} has been described in the literature. A crude theoretical estimate of the value of the lifetime by the extreme single-particle formula (1) of Weiskopf gives a mean life of about 10^{-12} seconds. Typically E2 transitions have often been found to be somewhat faster than indicated by this estimate. This would seem to indicate that the state would be one quite well suited to investigation by use of a Doppler shift method. It therefore seemed reasonable to try to observe the effect on the γ—ray energy produced by stopping the Be^{10} recoils in a metallic foil with a slowing-down time of the order of a few times 10^{-13} seconds. It was decided to look for a difference in γ—ray energy observed at a fixed angle while allowing the Be^{10} to recoil into two different media, a metallic foil, or vacuum. This energy difference is just the difference in the Doppler shifts of the γ—ray energy in the two media. This arrangement was chosen to avoid the uncertainty and additional complications which would have been introduced by changing the angle of the γ—ray detector in order to measure the Doppler shift in a single stopping medium. In order to separate the desired 3.37 Mev γ ray from the γ rays

produced by other reactions, a coincidence arrangement was used which at the same time also served to select a well defined Be^{10*} recoil velocity. This feature also greatly simplifies the analysis of the experiment.

Previous investigations (2,3) had already established an upper limit to the lifetime of the 6.14-Mev 3^- state of O^{16} by use of the recoil technique (4). In addition a lower limit to the lifetime had been established by use of the Doppler shift technique (2). These two limits together gave for the half-life, $t_{1/2}$, the range: 5×10^{-12} seconds $\leq t_{1/2} \leq 10 \times 10^{-12}$ seconds.

Earlier attempts (5) in this laboratory to measure the O^{16} lifetime had demonstrated the necessity for placing the target on a rigid backing, since thin foils, although they had the advantage of allowing one to use forward angles and thus obtain correspondingly higher recoil velocities, fluttered sufficiently under bombardment to mask any effect of a very short lifetime. The present experiment was therefore designed to use a target evaporated onto a rigid metal backing and the decay of the recoils in the backward hemisphere was then studied for evidence of an effect due to a small but non-zero lifetime. Earlier attempts to measure this lifetime made use of foils cemented over the target but no satisfactory method of cementing the foils onto the target without subsequent blistering under bombardment was found. Therefore a metallic layer evaporated over the target was used to stop the recoils, thereby providing a means for calibration of the apparatus. With these improvements in the target arrangement and with further improvements in collimation over that used in the

earlier experiment it was felt that the technique could be used down to the order of a few times 10^{-12} seconds as was known to be required from the previously established limits.

II. DETERMINATION OF AN UPPER LIMIT TO THE LIFETIME OF THE 3.37-Mev 2^+ STATE OF Be^{10} BY A DOPPLER SHIFT METHOD

A. Experimental Apparatus and Procedure

1) Choice of experimental approach - general

There are several possible experimental arrangements for determining the lifetime of an excited gamma-emitting state through use of the Doppler effect. These can be roughly described as follows:

One can bombard a target, stop the recoiling nuclei in some material, and then simply measure the γ-ray energy as a function of angle relative to the initial beam direction. A knowledge of the angular distribution of the recoil nuclei is then necessary to enable one to infer the lifetime from the energy measurements. This latter requirement can be eliminated if the recoil velocity vector is also determined, for example, by requiring coincident detection of the γ ray with the residual particle produced in a two body breakup of an intermediate nucleus.

One can instead, change the material in which the recoils are stopped and measure the difference in energy of the γ rays for different materials at some convenient and fixed angle. Again, a coincidence selection of the velocity of the recoil nucleus can be used to eliminate the necessity of knowing the angular distribution of the recoil nuclei.

A preliminary study of the feasibility of making a Doppler shift measurement of the 3.37-Mev γ ray of Be^{10} without the use of a coincidence arrangement was first made. A Be^9 target about 10 kev

thick to 1-Mev protons evaporated onto a chromium plated brass backing was bombarded with 2.76-Mev deuterons. These were provided by the Kellogg Laboratory 3 Mv-electrostatic generator and were energy selected by means of an electrostatic analyser. The γ rays produced were detected in a 1.5-inch by 1.5-inch cylindrical NaI(Tl) scintillation crystal. The resulting differential pulse height spectrum gave little or no evidence of a 3.37-Mev γ ray, because of a high yield of neutron capture γ rays and C^{13} γ rays produced by the $C^{12}(d,p)C^{13*}$ reaction on carbon contamination of the target used. Attempts to suppress the unwanted γ-ray background by neutron shielding were not successful. This led to the decision to use a coincidence arrangement by which one might hope to eliminate, or at least significantly reduce, the unwanted contributions to the γ-ray spectrum. As noted above this much more difficult approach does have the additional advantage of making it unnecessary to know the angular distribution of the recoil nuclei.

As a preliminary to the design of the target chamber and the coincidence arrangement the yields and other relevant properties of the various particle groups from Be^9 plus deuterons were studied in an angular distribution target chamber previously constructed by Marion (6). Typical differential pulse height spectra observed with thin CsI(Tl) crystals are shown in Figures 1, 3, and 4. These particle groups were observed at 2.755-Mev incident deuteron energy (Figure 1) and at 3.024-Mev incident deuteron energy (Figures 3 and 4) with a 0.0015-inch Al absorber in front of the scintillator. The target used, a thin unsupported foil of about 10 μ gm/cm^2 thickness, evidently had considerable carbon and oxygen impurity as

indicated by the carbon and oxygen groups present. The absorber foils used in this study were sufficiently thick to stop the elastically scattered deuterons as well as all α-particle groups from berylium, carbon, and oxygen. The identification of the groups was made upon an energy basis and also upon the basis of their behavior with various foil thicknesses. That this identification is correct is very well supported by the CsI(Tl) pulse height response vs. particle energy calibration curve, shown in Figure 2, constructed from the assumed identification and known Q-values. From this study it was found that a quite pure group of p_1 protons could be separated from the various unwanted groups at an angle of 160° or greater to the beam direction, with appropriate stopping foils and a deuteron beam energy of about 3 Mev. The large back angle for the protons and the high beam energy were also desirable for an additional reason: namely to provide as large a velocity as possible to the recoiling Be^{10*} nuclei. The recoil velocity actually attained in this experiment was $1.884 \times 10^{-2} \times c$ or 5.65×10^8 cm/sec. The observed yield of the proton group corresponding to the 3.37-Mev state of Be^{10} was of the order of 100 per μC at E_1 = 3 Mev and $\theta = 160^\circ$ for the 10 μ gm/cm^2 target. The proton detector solid angle was about 1.72×10^{-3} steradians, which for the given target thickness indicates a proton yield of about 5.8×10^4/sec/μamp/ster. Thus, for purposes of rough orientation, a proton detector of 0.03 steradian solid angle and a γ-ray detector with a solid angle of about 0.1 steradian (and therefore an overall detection efficiency of about

$\frac{0.1}{4\pi}$ x 0.06 = 5 x 10^{-4}) would yield about 1 coincidence/sec/μamp of beam current. The target chamber and target arrangement which were constructed with these considerations in mind is described in the following section.

2) The Target Chamber Design

A schematic diagram representing a horizontal section of the complete target chamber arrangement is shown in Figure 5 and the proton detector assembly is shown in a more detailed view in Figure 7. Since the preliminary work already mentioned had indicated that it would be desirable to detect the protons at a back angle relative to the incoming direction beam of the order of 160° or greater and, since larger angles would also give larger Doppler shifts, it was decided to choose this angle to be as large as could be practically arranged. An angle of 170° was finally chosen and with a 3/4-inch diameter proton detector crystal it was found possible to obtain a solid angle of approximately 0.03 steradians centered at that angle.

In general outline the target chamber consisted essentially of a cylindrical tube, which housed the proton detector assembly, and a beam entrance tube inclined at an angle of 10° to the main tube. The axis of the beam tube intersected the axis of the main tube at the target position. Another tube, which effectively formed a continuation of the beam entrance tube, extended beyond the target itself and formed the beam stopper and also a Faraday cage for the charge collected. The main target chamber is a 2.25-inch O.D. lucite tube with a 1/4-inch nominal wall thickness.

The 1.75-inch nominal inside diameter was reamed out at one end to an inside diameter of 1.812 inches in order to provide a smooth and continuous fit for the proton detector assembly. The opposite end of the main tube was capped with a lucite plate cemented in place. Another lucite tube 3.875 inches long was cemented into the end cap. The beam catcher, a tantalum lined brass tube, was then fitted into this tube with the vacuum seal being made by an O-ring placed in the brass tube. This provided a distance of about 4.1 inches between the target and the point where the beam was stopped. The side tube, which formed the beam channel tube, was also of lucite with an O.D. of 7/8 inch, an I.D. of 1/2 inch, and an overall length of about 6.125 inches. This was cemented to the main target chamber tube in line with a 1/2-inch hole, which had been drilled through the wall of that tube at an angle of 10°, and placed so that its axis interesected the desired target position and was coincident with the axis of the beam catching tube beyond the target. The end of this beam entrance tube, which also formed the vacuum pumping line, was fitted with an O-ring which allowed another tube to be inserted to make the connection to the electrostatic accelerator vacuum system.

The target position is indicated in Figure 5 and the arrangement is shown in more detail in Figure 6 which represents a vertical section through the center line of the main target chamber tube. The target holder was mounted on the end of a 1/8-inch rod which allowed vertical adjustment and rotation of the target to be performed from outside the vacuum system. The target rod was positioned to intersect the target chamber tube axis at the

correct point by a cap which in turn fitted into a lucite plug cemented to the main tube. The vacuum seals were made by O-rings. The target holder consisted of a small brass block with a 3/8-inch hole drilled through it, and a small 0.015-inch thick tantalum plate with a matching hole which could be used to clamp a foil in place. The same clamp was also used to mount a small piece of quartz at the bottom of the holder so that by raising the supporting rod the beam position and size could be observed visually.

The target itself was a thin layer of Be^9 evaporated from a tantalum boat onto a nickel foil of 5000 A^o thickness. An additional and identical piece of nickel foil was placed at a distance of about 0.015 inch from this foil and on the same side of that foil as was the berylium target layer. This arrangement then provided identical beam conditions at the target layer for both orientations of the target with respect to the beam. In one position the Be^{10} recoils moved out into the vacuum between the foils and in the other the recoils moved into the nickel backing until they were stopped.

3) The Proton Detector Assembly

The proton detector assembly, shown in place in Figure 5, (and in greater detail in Figure 7), is a scintillator crystal and a photomultiplier tube encased in a cylindrical brass holder which serves as a light shield. The particles are admitted through a 0.812-inch hole whose axis coincides with that of the brass cylinder itself.

The photomultiplier tube chosen for this purpose was the Dumont type 6467. This has the electrical and photoelectric properties of the more widely used Dumont types 6291 and 6292 but is considerably smaller, an important feature for this application. The nominal O.D. of the photomultiplier tube is 1.25 inches and the design and dimensions of the housing assembly were adjusted to this dimension. A lucite cylinder of about 1/8-inch wall thickness was placed around the photomultiplier tube to insulate it electrically from its metal housing. This insulation was desirable because the photomultiplier was to be operated with a negative high voltage cathode supply and the experience of others had indicated that the glass envelope of the tube, held at a high internal voltage with respect to metal in contact with its outside surface, would often give rise to serious noise pulses, presumably from electrical breakdown through the glass. This insulator sleeve was in two sections with an O-ring being placed around the photomultiplier tube between the two sections to provide a vacuum tight seal between the tube and its housing.

The proton scintillation detector was a 3/4-inch diameter piece of CsI(Tl) cut and water polished down to a thickness of about 0.006 inch. It was mounted in a recess 0.010 inch deep in the front end of a 1/2-inch long lucite light pipe. The light pipe was rounded at the front end and then gradually transformed into a taper leading back to a 1-inch diameter at a point where it ended in a flange 1.25 inches in diameter and about 0.063 inch in thickness. The 1-inch diameter of the light pipe at the back end roughly matched the nominal 1-inch diameter of the photosensitive area of

the photomultiplier tube. The outer edge of the flange fitted into a shoulder in the brass housing piece and formed the forward stop for the photomultiplier tube and light pipe assembly which was held in place by reason of the vacuum existing in the target chamber. The light pipe also provided the electrical insulation of the forward end of the photomultiplier since the outside edge of its flange was continuous with the lucite sleeves mentioned above. The optical couplings for both the scintillator-light pipe interface and light pipe-photomultiplier interface were made with Dow-Corning "200" one-million centistokes silicone fluid. Aluminum foil of 200 μ gm/cm^2 thickness was placed over the scintillator and the forward end of the light pipe in order to provide the maximum possible light collection efficiency for the proton detection system.

When the proton detector assembly was in place the scintillator was at a distance of about 3.812 inches from the target and thus provided a proton detector solid angle of approximately $\frac{\pi}{4}\left(\frac{3}{4}\right)^2 \Big/ \left(\frac{61}{16}\right)^2$ (= 0.0304) steradian or roughly one four-hundredth of the full sphere. The front end of the photomultiplier housing was covered with a tantalum disk with a 3/4-inch aperature to admit the protons. This disk held in place a 0.0015-inch thick Al absorber foil which the previous studies had indicated to be appropriate. A channel for vacuum pumping of the front end of the photomultiplier housing was placed beneath the tantalum disk. This was made circuitous and was also painted black to prevent the admission of light into the photomultiplier housing. The disk extended across most of the beam entrance aperture and a 0.111-inch hole was

drilled through the disk to provide for the passage of the deuteron beam and thus at the same time to provide a means for defining the beam and its alignment.

4) The γ—Ray Detection System

A 1.5-inch diameter by 1.75-inch long NaI(Tl) scintillation crystal was used for detecting the γ rays. This was optically coupled with the one-million centistokes viscosity Dow-Corning "200" silicone fluid to an R.C.A. end-window type 6655 high gain photomultiplier tube. This assembly was placed directly adjacent to the target chamber on the opposite side of the beam tube from the proton detector assembly, with its axis in the horizontal plane defined by the deuteron beam and the proton detector axis (see Figure 5). The γ—ray detector axis, which, projected through the target position, formed a backward angle of 156.5° relative to the incoming deuteron beam direction. The front end of the photomultiplier and detector assembly was located at about 4.375 inches from the target position which placed the median plane of the NaI(Tl) crystal at about 5.625 inches from the target thus giving a γ—ray detection solid angle of about 0.056 steradian or roughly 1/230th of the full sphere.

Both photomultipliers were magnetically shielded with mu-metal cylinders and an additional iron cylinder was placed over the target chamber section containing the proton detector photomultiplier. The shields for the proton detector had to be split along one side to allow for the beam entrance tube and it appeared that the compounded shield of iron and mu-metal was satisfactory

even though it did not form a continuous cylindrical covering for the photomultiplier tube. Partial shielding of the γ-ray detector against unwanted background radiation was provided by surrounding the whole assembly with several inches of lead arranged so that essentially only a conical hole was left between the target position and the NaI(Tl) crystal. This aperture was in turn filled with BC_4, contained in a cloth sack, in an attempt to provide some shielding against neutrons produced primarily at the target and in the beam catching tube. The front end of the crystal assembly was covered with a graded shield of tantalum and tin in order to eliminate x rays and very low energy γ rays produced in the target chamber. A large amount of positron activity, presumably N^{13} produced by the $C^{12}(d,n)N^{13}$ reaction, was always present. A partially successful attempt to shield out some of the resulting anihilation radiation was made by filling all the space in the target chamber not needed for the passage of any of the beam, γ rays, or particles to the proton detector with lead cylinders having the requisite channels machined into them. This seemed to reduce the anihilation radiation background and one would also expect it to help shield the proton detector from protons scattered from the back end of the chamber. A lead sleeve was also fitted into the beam stopping tube to help suppress further γ rays and neutrons originating at the point where the beam was stopped. Protons originating in this area were completely isolated from the proton detector, except for a small amount of double scattering which would be allowed by this particular geometry, by the intervening beam stopping tube and also by the lead piece surrounding the target position.

5) The Design and Operation of the Electronic Apparatus

A simplified schematic diagram or block diagram of the overall system used is shown in Figure 8. The general coincidence arrangement was of the type that has come to be known as the fast-slow coincidence scheme. All pulses from the proton detector were put into fast coincidence with all the pulses from the γ-ray detector. Pulses from the anodes of the two photomultipliers were fed into two limiters which produced output pulses of a standard height and width for all input pulses greater than about 5 volts. These were fed to a coincidence detector which selected events corresponding to an overlap in time, or coincidence, of the two input pulses. This operation thus accomplished the high resolution time selection of protons and γ rays in coincidence and constituted the "fast" part of the fast-slow system.

The proton spectra contained a great number of particles of energy comparable to and greater than the group of interest all of which of course produced the standard limiter output pulses that were fed to the fast coincidence mixer. An additional selection on the protons was therefore made by requiring that the proton pulses have a pulse height within a given range appropriate to that for protons leaving the Be^{10} nucleus in its first excited state. This "side channel" requirement was accomplished by amplifying the pulses which appeared at the 7th dynode of the proton detector photomultiplier and using a differential discriminator to select thosepulses within the desired pulse height range. The output of the differential discriminator was then fed into a "slow coincidence" mixer along with amplified output pulses from the fast

coincidence mixer. The output pulses from the slow coincidence mixer were then used to open a "gate" in a 100 channel pulse height analyzer into which all amplified pulses from the 7th dynode of the γ-ray detector photomultiplier were fed.

The photomultiplier dynode high voltage distribution resistor and capacitor filter strings were enclosed in a small unit built around the photomultiplier tube socket and physically separate from the pre-amplifier and limiter chassis. The photomultiplier anode and seventh dynode outputs were then connected to the pre-amplifier chassis through short lengths of coaxial cable as was the high voltage supply.

The schematic diagram of Figure 9 shows the limiter and pre-amplifier circuit which was used for both the proton and γ-ray detector outputs. Western Electric type 404A pentode tubes, with a $g_m \sim$ 20mA/volt, were employed as limiters. The plate loads of these tubes were short lengths of the 950-ohm R.G. 65/U coaxial delay line. The termination of these delay lines was provided by germanium diodes which clipped the negative going reflection while allowing the positive going plate to rise to the full voltage value given by the product of the total current switched off and the characteristic impedence of the delay line pulse shaper. These limiter pulses, which were about 40mμ seconds wide at their base as measured on a Tectronix model 517 oscilloscope and of about 15 volts amplitude, were then fed to a cathode follower cable driver, the Western Electric type 417A high g_m triode. The cathode follower outputs were then fed via appropriate lengths of R.G. 114/U 185-ohm coaxial cable to the fast coincidence mixer.

The fast coincidence mixer used, see Figure 10, was essentially a modification of a design developed by G. C. Neilson and D. B. James (5). A 6BN6 gated beam tube was used for the basic coincidence detection unit. This tube has two separate grids either one of which, when biased below a certain voltage, will deflect the cathode current away from the plate. However, when both grids are made positive by about 1 to 2 volts the full current is allowed to pass directly to the plate. This current pulse produces an output signal voltage across the plate resistor approximately proportional to the overlap in time of the two grid pulses. The fast coincidence resolving time was typically of the order of 20 to 30 x 10^{-9} seconds, depending on the degree of time-overlap required. This output was inverted by an amplifier stage and fed to a second amplifer stage which clipped the pulses to a width of 1 μ second, and finally to another amplifier which brought the coincidence output pulses up to a level of about 20 volts as required by the slow coincidence mixer.

It was found impossible because of the appearance of a large amount of tube noise at about 1600 volts and higher to use the proton detector photomultiplier at a voltage sufficiently high to operate the limiter directly. To overcome this the anode output pulse of the 6467 photomultiplier was amplified first by three Hewlett-Packard distributed amplifiers in cascade and then fed into the limiter unit. Approximately 75 feet of R. G. 114/U coaxial cable were introduced between the limiter and fast coincidence mixer in the γ-ray channel to compensate for the difference in photomultiplier transit times and to allow for the additional delay introduced into the fast proton channel by the three distributed amplifiers. The remainder of the electronic apparatus was of conventional design.

6) Data Taking Procedure and Typical Results

A deuteron beam current, typically about 0.15μ amp. was employed to produce the Be^{10} recoils for this experiment. This was provided by the Kellogg Laboratory 3-Mv electrostatic generator and the beam was regulated in energy by an electrostatic analyzer at a value of about 3.092 Mev. The resulting γ-ray spectrum was accumulated in the 100 channel analyzer usually for a period of about one hour for a given target orientation. The spectrum was read out digitally and the target was then reversed and the procedure repeated again, with a delay of from 5 to 10 minutes between the periods of accumulation of the γ-ray spectrum for the recording of the spectrum. A typical complete set of such spectra would consist of from 3 to 5 such accumulations for each of the two target orientations. Figures 11 and 12 show typical γ-ray spectra resulting from one hour runs corresponding, respectively, to the Be^{10} recoiling into vacuum and into nickel.

B. Analysis of the Data and Discussion

Composite spectra for each of the two target orientations were made up by summing together all the corresponding individual spectra of a given set. Two such averaged spectra, corresponding to recoils into vacuum and nickel respectively, are shown in Figures 13 and 14 and are shown superimposed in Figure 15. The shifts in energy indicated by these spectra and others similarly constructed were estimated both by a visual comparison and by an analysis of their centroid positions. The estimated shifts for the individual sets of spectra found by a visual comparison are tabulated in Table I. The drift correction was made by measuring the position of the Th C" 2.62-Mev γ-ray full energy peak before and after the complete set of runs and assuming that the shift was linear with time. The average shift indicated by this visual estimation for all such spectra regarded as satisfactory for analysis was + 0.022 $\pm$ 0.321 channels, where the full energy peak of the 3.37-Mev γ ray was in channel 85 $\pm$ 1. The average value was constructed by weighting the individual sets according to the inverse squares of the errors indicated for each, while the overall error indicated is the variance of the shifts of these sets from this average, constructed by weighting according to the number of spectra in each set. The maximum possible shift (corresponding to a lifetime long compared with the stopping time) that could have occurred for the actual experimental configuration and beam energy used was 1.42 $\pm$ 0.05 channels.

TABLE I

Shifts Found Visually for the Individual Sets of Spectra

Number of Set	Number of Spectra	Shift (Channels)	Correction For Drift (Channels)	Corrected Shift (Channels)
1	7	-0.1 ± 0.4	$+0.0$	-0.1 ± 0.4
2	8	-0.3 ± 0.6	-0.1	-0.4 ± 0.6
3	10	$+0.1 \pm 0.4$	$+0.08$	$+0.2 \pm 0.4$
4	7	$+0.5 \pm 0.6$	$+0.0$	$+0.5 \pm 0.6$
5	9	-0.2 ± 0.4	$+0.0$	-0.2 ± 0.4
6	2	$+0.4 \pm 0.8$	$+0.12$	$+0.5 \pm 0.8$

The estimated shifts determined from an analysis (see Appendix II) of the centroid positions of these spectra are shown in Table II. The average shift indicated by this set of estimates is -0.54 ± 0.52 where the individual measurements have been weighted

Table II

Shifts Found From an Analysis of the Centroid Positions of the Individual Sets of Spectra

Number of Set	Number of Spectra	Shift (Channels)	Correction For Drift (Channels)	Corrected Shift (Channels)
1	7	-1.50	+0.0	-1.50
2	8	-0.21	-0.1	-0.31
3	10	-0.12	+0.08	-0.04
4	7	-0.12	+0.0	-0.12
5	9	-0.78	+0.0	-0.78
6	2	-1.10	+0.12	-0.98

according to the number of spectra in each set and the error indicated is again the variance of the individual values from their mean. The shift indicated by this method is negative. However it is only about one standard deviation from small positive values of the shift and the errors corresponding to the two estimates overlap quite well. Using the shift constructed from visual estimates, since this will give the largest estimate of the upper limit to the lifetime of the two methods, the relative shift is determined to be less than about 0.343/1.42 (= 0.242) of the full Doppler shift available for the experimental arrangement used. The mean life, τ, can be related to the relative shift, $\Delta E_{obs.}/\Delta E_{max}$, and to the slowing down time, , of the recoil nucleus in the stopping material involved by the relation (see Appendix I)

$$\frac{\tau}{\tau + \alpha} = \frac{\Delta E_{obs}}{\Delta E_{max}} \quad .$$

From the observed data only the inequality $\frac{\tau}{\tau+\alpha} \leq 0.242$ can be inferred and one obtains from this an upper limit of $0.32\,\alpha$ for τ.

No data on the stopping cross section for Be ions at low energies has been published. Therefore a crude estimate of α for Be^{10} in nickel was made by first making an interpolation in stopping cross section, linearly with Z at a given value of ion velocity, between measured values for He^4 and B^{11} in air (7, 8, 9, 10). Some lithium-ion data for air is available but does not extend to a sufficiently high energy to be very useful. The data on He^4 and B^{11} are the nearest to Be^{10} (in Z) that one has and the linear interpolation is of course a very uncertain procedure. Data on carbon ions in air, for this same velocity, is also available (9, 10) and

an interpolation linear in Z between C and He gives for B a stopping cross section value within about 3 percent of the measured value which, though perhaps largely fortuitous, seems to provide some empirical justification for the procedure. This estimate of the ratio of stopping cross section for Be and He ions in air was then assumed to be the same for copper. He^4 stopping cross sections are not available at this energy for nickel but at higher energies those for copper and nickel are very nearly the same (10, 11). The final estimate of stopping cross section for Be^{10} in nickel was then computed using the already described ratio for Be^{10} and He^4 and using the stopping cross section (at the appropriate energy) for He^4 ions in copper (10, 11). The estimate for α obtained in this way (see also Appendix I) is about 4.9×10^{-13} seconds. This value coupled with the uncorrected limit observed for the Doppler shift gives an upper limit for τ of 1.6×10^{-13} seconds.

This estimate of the limit to the 3.37-Mev state lifetime is subject to several uncertainties. The photomultiplier used in the γ-ray detector exhibited a gain dependence on counting rate. This was of such a magnitude as to give a change of as much as 4 or 5 percent in pulse height between the condition of a very low counting rate and a counting rate of the order of 10^5 per second as used in this experiment. In order to minimize such effects a γ-ray source was used for several hours previous to a run to bring the photomultiplier to an approximate equilibrium. The beam current was also held as nearly constant as feasible during the ensuing bombardment in order to reduce fluctuations and drift in photomultiplier gain.

One would hope that these precautions, coupled with the successive alternation of target orientation, and a small correction for any residual drift occurring during the complete set of runs, would reduce the uncertainty due to this feature to an acceptable level. Most of the observed dispersion evident in the shift measurements is believed, however, to be due to an imperfect compensation for the effects of the photomultiplier gain drifts. A further uncertainty in the estimates of Doppler shift results from actual impurities in the observed coincidence γ-ray spectrum. Even the coincidence-gated γ-ray spectrum still exhibited some evidence of γ rays other than the 3.37-Mev γ ray, presumably from random coincidences. These were primarily the carbon 13 γ rays and neutron capture γ rays. In the typical ungated γ-ray spectrum the 3.09-Mev C^{13} γ ray ranged from nearly equal intensity to perhaps one and one-half times the intensity of the 3.37-Mev Be^{10} γ ray.

In the coincidence gated spectrum the C^{13} 3.09-Mev γ-ray content seems to be reduced by a factor of at least 5 relative to the 3.37-Mev γ-ray real coincidence spectrum. In the ungated γ-ray spectrum there are at this deuteron energy, according to Meyerhof and Chase (12), about 5 times as many 3.37-Mev γ rays produced by cascade decay of higher excited states of Be^{10} as are produced directly by the (d,p_1) reaction. These cascade 3.37-Mev γ rays would also appear in the coincidence-gated γ-ray spectrum as random coincidences and should contribute about equally with the C^{13} γ rays. The C^{13} 3.09-Mev γ-ray transition is known to be an E1 transition and should be fast enough to give no observable difference in Doppler shifts for the two positions of the target,

and hence, this γ ray would serve only to reduce the spectrum shift as calculated by the centroid method. The shift shown by the 3.37-Mev γ rays produced by cascade decay would be considerably less than that resulting from the directly produced 3.37-Mev γ rays. This effect would also tend to reduce (for both methods of calculation), the observed difference in Doppler shift. In view of these effects the possible spectrum shift, which would have been exhibited by a pure 3.37-Mev γ ray produced only by Be^{10*} nuclei recoiling in the required direction from p_1-protons, could be perhaps as much as 50 percent larger than the observed shift. This results in a corrected estimate of 2.8×10^{-13} seconds for the upper limit to the mean life. The transit times of the Be^{10} nuclei within the target layer would be of the order of a few times 10^{-15} seconds and need not be considered in this analysis since the lifetime limit being inferred is much longer than this. In view of all these effects a final value of 3.0×10^{-13} seconds for the upper limit to the 3.37-Mev Be^{10} state mean life is quoted, which probably should be considered as an estimate good to something like the 50 percent confidence level.

The photomultiplier gain instability has been the chief problem in this experiment and further study to find a more stable photomultiplier would be necessary to make a decisive improvement over the present experiment. A faster coincidence system could perhaps be used if a faster scintillator, for example NaI(Tl) or a plastic scintillator, were used for the proton detector. This would allow a cleaner γ-ray spectrum to be attained with the resulting improvement in the certainty of analysis. For situations where it is not necessary to select γ rays in a coincidence arrangement,

the data collection times and the resulting gain drift problems would be much reduced. For these cases then, one would probably best avoid the coincidence method while the alternation of recoil stopping material as used here would still seem to be a desirable and useful approach.

C. Comparison of the Observed Limit to the Mean Life of the 3.37-Mev State With Some Theoretical Estimates

1) The Extreme Single-Particle Estimate of the Lifetime

The single-particle mean life for this E2 transition given by the Weisskopf formula (1) is about 10^{-12} seconds. This value was taken from a nomogram constructed by Montalbetti (13) for the use of that formula and assumes for the radium parameter, R_o, a value of 1.5×10^{-13} cm. However the recent experimental work at Stanford (14) on nuclear scattering of electrons from Beryllium indicates that a radius parameter of about 1.89×10^{-13} cm would be more nearly correct. This radius decreases the estimated single particle mean life to about 4×10^{-13} seconds. The experimentally determined limit to the mean life is comparable to but somewhat shorter than the single-particle limit.

2) The "α-Particle Core" Model Estimate of the Lifetime

The spins and parities of the ground and 3.37-Mev states of Be^{10}, 0^+ and 2^+ respectively, are such as to suggest the following model for these states. The Be^{10} nucleus, when in these two states, might be described as a Be^8 α-particle core plus two neutrons whose angular momenta are in both cases coupled to give zero. The first two rotational states of the Be^8 α-particle core would then provide the required angular momenta and parities for the ground state and first excited state of Be^{10} respectively. In addition the actual difference in binding energy of these first two rotational states in the Be^8 nucleus itself is about 2.90 Mev (15) and hence the assumed rotational core of Be^{10} could provide very nearly the correct energy difference for the first two states of the Be^{10} nucleus.

The binding energy induced by the two neutrons (8.477 Mev (15) relative to the Be^8 ground state) could well be very nearly the same for both states if as suggested by the model the α particles are relatively distinct structures for both states and this binding resulted primarily from the neutron - α interaction and neutron - neutron interaction.

A rough estimate of the γ-ray lifetime corresponding to such a model would then be given by a calculation of the γ-ray transition rate produced by the core alone, using for the required energy difference that of the Be^{10} states themselves. The transition rate would of course be somewhat suppressed from this calculated value since the neutron wave functions could not have a complete overlap in the two states involved in this transition. The α-particle core which is "imbedded" in the neutron cloud makes a transition from a 2^+ rotational state to the 0^+ ground state of the rotational series and hence a corresponding change must be induced in the neutron cloud which would be at least partially excluded from the volume occupied by the α particles.

If one uses a harmonic oscillator radial dependence in the wave function and adjusts the radial parameter to give the same r.m.s. value to the charge distribution radius of the core as was found for the Be^9 nucleus by the electron scattering experiments (14) one finds for the mean life a value of about 8×10^{-15} seconds. This value is incidently, the minimum lifetime that could be obtained with Z equal to 4 and with the assumed radial dependence of the charge distribution. The experimental upper limit to the lifetime is well above this value and hence the experiment is not able to decide whether or not this model should be taken seriously.

III. MEASUREMENT OF THE LIFETIME OF THE 6.14-Mev 3^- STATE OF O^{16} BY A RECOIL METHOD

A. Experimental Apparatus and Procedure

1) Mechanical and Electronic Apparatus

The apparatus, shown in Figure 16, consisted of a thick brass target block mounted on the end of a differentially threaded shaft by means of which the target could be moved parallel to the beam direction in small steps across a highly collimated γ-ray detector. The collimation arrangement consisted in part of a 1/8-inch thick plate of tungsten 2 inches wide by 7.5 inches long mounted on a rigid brass block normal to the beam direction and facing the incoming beam. The surface of the tungsten was an accurately ground flat face and one end was placed within about 0.050 inch of the target block. The remainder of the collimator consisted of two lead blocks of dimensions 2" x 4" x 6" mounted at the end of the tungsten face, opposite the target block. One of these blocks formed a continuation of the tungsten face, with its 4" x 6" face carefully adjusted to be in the same plane; the other lead block faced the first lead block with a separation from it of 0.006 inch at the end adjacent to the tungsten and 0.010 inch at the far end. The total length from the target to the end of the lead collimator was approximately 14 inches. The effective solid angle of the collimator was approximately 1.5×10^{-4} steradian. The target block itself was a thick carefully polished brass disk, 3 inches in diameter. This target backing was a few thousands of an inch smaller in diameter than the inside of the aluminum cylinder which formed part of the vacuum chamber. That section of the wall of the vacuum chamber which

separated the target from the nearby tungsten edge was about 0.02 inch thick and in addition approximately 0.02 inch separated the aluminum from the tungsten edge. This then made it possible to keep the total separation of the target spot from the adjacent edge of the tungsten at not more than about 3/32 inch. It was essential to keep this separation small in order to make the collimation system as effective as possible.

The differential screw assembly, shown schematically in Figure 16 and in more detail in Figure 17, was used to position the target plane relative to the plane of the tungsten collimator. This assembly included a hardened steel shaft with a threaded section of 48 threads to the inch. The shaft was fitted into a mild steel plate which in turn formed the back of the vacuum chamber and was rigidly bolted to the framework of the collimation system. The back plate had a hollow cylindrical section integral with the back plate extending back concentrically with the shaft. This section was threaded on the outside with 44 threads to the inch. A single bronze nut appropriately threaded to match these two threaded concentric cylinders was then fitted onto both the central shaft and the extension of the back plate. The shaft was prevented from rotating by an external clamp placed on its outer end. Rotation of the nut then provided a finely controlled motion to the central shaft, with effectively 528 $(= (\frac{1}{44} - \frac{1}{48})^{-1})$ threads to the inch. All the threaded sections and sliding parts were very carefully machined and fitted together with a minimum of free play. This helped assure uniformity of motion and reproducibility of position of the target. During measurements the target was always moved in one direction only, from a position

ahead of the range of positions actually being studied. Furthermore atmospheric pressure on the cross section of the shaft provided a uniform load of about 26 lbs. working against the differential screw. This reduced any tendency of the shaft to move erratically because of the friction of the shaft against the inside cylindrical wall of the back plate and its extension or the O-ring contained in that wall. Tests performed with a simulated atmospheric load using a 0.0001-inch position indicator showed that this arrangement could position the shaft with a reproducibility of about 3×10^{-5} inch under the uniform conditions of the tests.

The other end of the vacuum chamber was capped by a brass plate into which two electrically heated evaporating furnaces were mounted. These permitted laying down either a target layer or an overlying metallic layer without mechanically disturbing the system. These furnaces were in the form of a tantalum boat for the target evaporation and a tungsten or tantalum wire for the evaporation of the overlying metallic layer of either gold or copper. In addition this plate contained a sylphon bellows which served both as the vacuum pumping outlet and as the beam entrance channel to the target.

The γ-ray detector consisted of a cylindrical 4-inch x 4-inch NaI(Tl) scintillation crystal which was mounted on a Dumont type 6364 5-inch photomultiplier placed immediately behind the lead collimator with its axis of symmetry directed toward the target. Conventional pulse amplifiers, discriminators, and associated electronic circuitry were used with this detector. The γ-ray pulses from the 4-inch x 4-inch crystal were amplified and fed to a 10 channel differential pulse height analyzer which accepted pulse heights

corresponding to energies in the range of about 4.5 Mev to 7.5 Mev. The γ-ray yield was also monitored by an independent 1.5-inch x 1.5-inch Na I(Tl) detector.

2) General Operating Procedure

The $F^{19}(p, \alpha_1)O^{16*}$ reaction at the 873-kev resonance provided the O^{16*} recoils. This resonance was chosen because of the favorable production of the 6.14-Mev state relative to the other two γ-ray emitting states at 6.9 Mev and 7.1 Mev, and also because of its large absolute cross section for the production of that state(15). It was also found that higher bombarding energies seriously increased the general background from the accelerator. The targets used were evaporated layers of CaF_2 8 to 30 kev thick for the 873-kev proton beam. Optimum results were obtained for a target thickness of about 15 kev.

Proton beam currents of one to two microamperes were ordinarily employed. The proton beam was provided by the Kellogg Laboratory 3-Mv electrostatic generator and a double focusing magnetic analyzer was employed for energy regulation of the beam. It was found feasible in typical operation to place the beam current within an area of about 1/32 inch x 1/16 inch, approximately 1/32 inch from the edge of the target block.

The typical experimental run consisted first in adjusting the screw to place the target far enough ahead of the edge of the tungsten collimator to give maximum counting rate, corresponding to the full transmission of the collimation system. The central shaft was then backed out in steps corresponding to 18° in rotation of the

nut in the regions where the counting rate was slowly varying, i.e. either well in front of the edge or well behind it. In going across the edge however, steps of 9° were taken, which corresponded to withdrawing the target in steps of approximately 4.7×10^{-5} inch. For the situation with only the target layer evaporated onto the target backing 3 to 5 such runs were made in this manner across the tungsten edge, where for each setting of the target position approximately 50μ coulombs of charge were collected. Then a copper layer about 150 kev thick to 1-Mev protons was evaporated onto the target surface and the procedure was repeated for 3 to 5 runs with as much as 100μ coulombs of charge being collected for each point. These will be referred to as the "recoil" and "no-recoil" runs, respectively, in the following discussion. (Figure 18 shows the raw data for such a group of "recoil" runs.) It was found that the individual runs within the "recoil" and "no-recoil" groups were in general quite reproducible as to shape, but sometimes were displaced relative to each other by distances $\sim 5 \times 10^{-5}$ inch. In addition the recoil and no-recoil groups of curves, between which the evaporation of the stopping layer was carried out, were often shifted relative to one another by about 10^{-4} inch. The causes of these shifts were not isolated, and will be discussed further in section C. However these effects were not seriously detrimental to the analysis of the data since the difference in shape of the recoil and no-recoil curves was the significant result of this experiment.

Four such complete sets of data were accumulated which were regarded as suitable for analysis. In addition however a considerable amount of data consisting of groups of recoil or no-recoil

runs alone was accumulated. These were individually consistent with the four sets of runs which were used but were not included because the recoil and no-recoil runs were taken at different times and may well have represented slightly different conditions as to target spot size, location, and etc. In analyzing the data, averages of the complete sets of runs were taken after first normalizing each individual run by the average monitor count appropriate to that run. A background equal to the normalized counting rate observed with the target well behind the tungsten edge, amounting to about 10% of the full transmission value, was then subtracted. The resulting curves were then normalized to the same arbitrary value at the essentially flat maximum of the curves which corresponded to the target being in front of the tungsten edge. One of these curves is shown in Figure 19. The theoretically constructed distribution of decays for different assumed values of the lifetime was then folded into the no-recoil curves and the resultant curves were then compared with the corresponding recoil curves, as is further described in section B. Such a comparison can be seen in Figure 23.

B. Analysis of the Data-General

The measurement of the lifetime of an excited nuclear state by the recoil technique requires a comparison of the experimentally observed decay distribution curves with the corresponding distribution curves calculated for various assumed lifetimes. One can proceed by first assuming an idealized collimation system in which the collimator is one sided and completely effective, i.e. all gamma decays occurring on one side of a given plane have, except for possible anisotropy in angular distribution, a fixed non-zero probability of detection. The number of γ rays detected by such a system will then be proportional to the number of γ rays emitted from within the half-space which is visible from the collimated detector and, for the conditions of this experiment, into a direction normal to the proton beam direction. The differential distribution of counting rate as a function of the relative displacement of the collimator and target layer must then be determined from the above integral distribution. These calculated distribution curves may then be folded into the experimental "no-recoil" curves, which actually measure the effectiveness of the collimation for a γ-ray source identical with respect to its γ-ray spectrum but with an effectively zero lifetime. The resulting curves will then represent the predicted "recoil" distribution for the various assumed lifetimes including automatically the effects which result from the actual imperfect collimation system used rather than any idealized system.

Using Figure 20 for reference, the idealized distribution curve may be derived as follows. Because of the center of mass motion and the energy loss of the recoiling nuclei in the target

and contaminating layers, as discussed below, the velocity is a function of the polar angle, θ, where θ is measured with respect to an axis along the proton beam direction and in the laboratory system of coordinates. For an excited O^{16} nucleus with a mean lifetime, τ, moving at an angle, θ, with respect to the beam axis and with a velocity, $v(\theta)$, the probability of decay between r and $r + dr$, where $r = v(\theta)t$, is then given by

$$P(r)\, dr = \frac{dr}{\tau v(\theta)}\, e^{-\frac{r}{\tau v(\theta)}} . \qquad (1)$$

Next one must find the probability that an excited O^{16} nucleus will emit a γ ray into a solid angle $d\Omega_\gamma$ at θ_γ, ϕ_γ, while recoiling into a solid angle $d\Omega$ at θ, ϕ. The polar angle is measured with respect to the proton beam axis, and since by symmetry this probability can only depend upon the relative azimuthal angle, ϕ will be measured from the p-γ plane so that $\phi_\gamma = 0$. This joint probability, or correlation function, will be written as follows:

$$U(\theta_\gamma, 0; \theta, \phi)\, \frac{d\Omega_\gamma}{4\pi}\, \frac{d\Omega}{4\pi} .$$

From the definition of the function, U, it follows that

$$\int_{4\pi} U(\theta, 0; \theta, \phi)\, \frac{d\Omega(\theta,\phi)}{4\pi} = W_\gamma(\theta_\gamma), \qquad (2)$$

where $W_\gamma(\theta_\gamma)$ is the p-γ distribution function, normalized so that

$$\int_{4\pi} W_\gamma(\theta_\gamma)\, \frac{d\Omega_\gamma}{4\pi} = 1.$$

In this experiment only γ rays emitted perpendicular to the proton beam axis were detected, i.e. only γ rays emitted at

$\theta_\gamma = \pi/2$. For brevity $U(\theta_\gamma = \frac{\pi}{2}, \phi_\gamma = 0; \theta, \phi)$ will be written $U(\theta,\phi)$. Knowing this correlation, $U(\theta,\phi)$, one may then find the probability $n(r, \theta, \phi)\, dr\, d\Omega$ of a γ ray, detected in a solid angle $\Delta\Omega_\gamma$ perpendicular to the proton beam, being emitted from an excited O^{16} nucleus recoiling into a solid angle $d\Omega$ at angles θ, ϕ and decaying between r and $r + dr$. This probability is

$$n(r,\theta,\phi)\, dr\, d\Omega = \frac{dr}{\tau v(\theta)} e^{-\frac{r}{\tau v(\theta)}} U(\theta,\phi) \frac{d\Omega}{4\pi} \frac{\Delta\Omega_\gamma}{4\pi} . \qquad (3)$$

Changing variables to $z = r \cos\theta$, and $\mu = \cos\theta$, the following integral probability is found:

$$N_{\pm}(a,\infty) = \pm \frac{\Delta\Omega_\gamma}{4} \int_0^{\pm 1} \bar{U}(\mu)\, e^{\mp \frac{a}{\mu \tau v(\mu)}} \frac{2\pi\, d\mu}{4\pi} . \qquad (4)$$

$N_{\pm}(a,\infty)$ is the probability of an excited nucleus decaying at a normal distance $|z| \geq a$ from the target plane, and emitting a ray into a solid angle $\Delta\Omega_\gamma$ perpendicular to the proton beam, the positive sign referring to recoils in the direction of the incident proton beam and the negative sign to recoils in the backward direction. $\bar{U}(\mu)$ is the correlation function averaged over the azimuthal angle of the recoiling nuclei, i.e.,

$$\int_0^{2\pi} U(\mu,\phi)\, d\phi = 2\pi\, \bar{U}(\mu) .$$

In the present experiment F^{19} was bombarded with 873-kev protons which also excite the second and third γ-ray emitting states of O^{16} at 6.9 and 7.1 Mev. The γ-ray detection apparatus could not resolve the 7-Mev radiation from the 6-Mev radiation with

which this experiment was concerned. The branching ratio, $N_1/(N_1 + N_2 + N_3)$, has been measured at this resonance (16,17,18), and was taken to be 0.70. Therefore if N is the total number of O^{16} nuclei produced in these three states, then $N_1 = 0.70\ N$ and $N_{2+3} = 0.30\ N$, where N_1 is the number excited to the 6.1-Mev state, and N_{2+3} is the number excited to the 6.9- and 7.1-Mev states. Lifetime limits have been measured for the latter two states as follows: $t_{1/2} \leq 1.7 \times 10^{-14}$ seconds for the 6.9-Mev state and $t_{1/2} \leq 8 \times 10^{-15}$ seconds for the 7.1-Mev state (19). More recent measurements (20) give $t_{1/2} = (8.3 \pm 0.2) \times 10^{-15}$ seconds and $t_{1/2} = (6.9 \pm 0.2) \times 10^{-15}$ seconds for the 6.9-Mev and 7.1-Mev states respectively. These two states then decay more than two orders of magnitude faster than the 6.1-Mev state, and therefore, within the linear resolution of the apparatus, simply add to the γ-ray yield from the target layer.

In this experiment the target backing stopped the excited O^{16} nuclei recoiling in a forward direction within a distance short compared with the linear resolution of the apparatus and therefore these forward recoils also contributed only to the γ-ray yield from the target layer. Combining the above results, the following expressions are found for the number of γ rays emitted perpendicular to the proton beam into a solid angle, $\Delta\Omega_\gamma$, from normal distances $-z \geq a$, from the target layer itself, and for the total number:

$$N_{-}(a,\infty) = N \frac{\Delta\Omega_\gamma}{4} \left[0.70 \int_{-1}^{0} e^{+(a/\mu\tau v(\mu)} \bar{U}(\mu) \frac{2\pi\, d\mu}{4\pi} \right], \qquad (5)$$

$$N_{target} = N \frac{\Delta\Omega_\gamma}{4\pi} \left[0.70 \int_0^1 \bar{U}(\mu) \frac{2\pi d\mu}{4\pi} + 0.30\, W_\gamma^{2+3}(\tfrac{\pi}{2})\right], \qquad (6)$$

$$N_{total} = N_{target} + N_{-}(0,\infty)$$

$$= N \frac{\Delta\Omega_\gamma}{4\pi} \left[0.70\, W_\gamma^{1}(\tfrac{\pi}{2}) + 0.30\, W_\gamma^{2+3}(\tfrac{\pi}{2})\right] . \qquad (7)$$

Sanders (21) has measured the $(p, \gamma_2 + \gamma_3)$ angular distribution at the 873-kev resonance, and Seed and French (16) have calculated it. From these authors the correlation was taken to be $I^{2+3}(\theta_\gamma) \propto 1 + 0.34 \cos^2 \theta_\gamma$, leading to $W_\gamma^{2+3}(\frac{\pi}{2}) = 0.90$.

In the center of mass coordinate system the (γ_1, O^{16}) and the (γ_1, α_1) correlations will be the same since the α particles and the O^{16} nuclei recoil in opposite directions. In this coordinate system the (γ_1, α_1) correlation, averaged over the azimuthal angle, Φ_α, of the α particle, between a γ ray at $\Theta = \frac{\pi}{2}$, $\Phi_\gamma = 0$, and an α particle at Θ_α is given by

$$\bar{U}(\Theta_\gamma = \tfrac{\pi}{2}, \Phi_\gamma = 0; \Theta_\alpha) = \frac{3}{1024} \frac{1}{1 + B^2} \times$$

$$\left[438 - 284 \cos^2 \Theta_\alpha - 138 \cos^4 \Theta_\alpha \right.$$

$$+ \sqrt{10}\, B \cos\beta \left\{ 17 + 291 \cos^2 \Theta_\alpha - 1185 \cos^4 \Theta_\alpha + 861 \cos^6 \Theta_\alpha \right\}$$

$$+ \tfrac{5}{2} B^2 \left\{ 165 + 388 \cos^2 \Theta_\alpha - 2196 \cos^4 \Theta_\alpha \right.$$

$$\left. \left. + 3864 \cos^6 \Theta_\alpha - 2205 \cos^8 \Theta_\alpha \right\} \right]. \qquad (8)$$

This correlation is derived from a knowledge of the angular momenta involved. $Be^{i\beta}$ was introduced to represent the relative amplitude and phase of the outgoing g-wave to d-wave α particles respectively. The derivation is also discussed in Appendix III.

The magnitude of $\cos\beta$ is determined from the analysis of the barrier factors (16), leaving the magnitude of B and the sign of $\cos\beta$ to be determined experimentally. Martin et al. (22) from a study of the (α_1, γ_1) correlation, combined with the results of the (p, α_1) distribution studied by Peterson et al. (23) and the results of the (p, γ_1) distribution studied by Sanders (21), found B = 0.85, $\cos\beta$ = + 0.242 with B = 0.2, $\cos\beta$ = -0.242 as possible but less likely. Seed and French (16) found B = 0.54, $\cos\beta$ = -0.245. In these calculations the values B = 0.85 and $\cos\beta$ = + 0.242 were used, but the other values give similar results, as will be shown later.

Having found $\bar{U}(\theta_\gamma = \frac{\pi}{2}, \Phi_\gamma = 0; \theta_\alpha)$, one may transform to the laboratory coordinate system, using Q = 1.98 Mev (15). and remembering that we are interested in the O^{16*} recoils. The resulting correlation is defined as $\bar{U}(\mu)$ where $\mu = \cos\Theta$ and Θ is defined in the laboratory system.

The O^{16} recoil velocity dependence upon cos Θ may be calculated from the kinematics of the reaction and for backward angles is given approximately by the following relation:

$$v(\cos\Theta) = \frac{2.53}{1 - 0.291\cos\Theta} \times 10^8 \text{ cm/sec} \qquad (9)$$

A correction must be made for the reduction of velocity of the recoiling nuclei in the calcium fluoride target layer itself and also in an overlying layer of beam-deposited carbon. The overall average depth of production of the $F^{19}(p, \alpha_1)O^{16*}$ reaction within the CaF_2 target layer for all recoil runs was about 8 kev. In addition a layer of carbon was formed during each set of recoil runs with an average

total accumulated thickness of 9 kev. The average carbon layer existing during a set of recoil runs was then taken to be 4.5 kev thick. Taking the stopping power for protons in CaF_2 and C as 190 kev-cm^2/mg and 284 kev-cm^2/mg respectively (11), average thicknesses of roughly 0.04 mg/cm^2 of CaF_2 and 0.016 mg/cm^2 of carbon were found.

To calculate the velocity loss of the O^{16} recoils in traversing these layers a range-velocity curve for O^{16} in air was constructed from the data of Blackett and Lees (24). The Bragg-Kleeman rule (25) was then used to adjust the range scale to the two materials, calcium fluoride and carbon. This rule states that for a given particle the range is approximately given by $R_1 = \sqrt{A_1/A_o}\ R_o$, where R_1 and R_o are in units of mass per unit area.

An extrapolation by the Bragg-Kleeman rule over the rather greater range from the O^{16} data for air to copper gives a value for the range of O^{16} in copper too large by about 30 percent compared to the range computed from the relation, $R = \alpha v$, with a value for α(Cu) of $(1.8 \pm 0.2) \times 10^{-13}$ seconds (19) (measured at a velocity of 2.8×10^8 cm/sec). Hence the errors made in constructing the range-velocity curves in CaF_2 and C may be of the order of 15 to 20 percent.

From these curves the velocity loss in bringing the recoils out through the two layers successively could be determined for a series of angles, given the initial velocity of the ion as determined from the reaction dynamics. The results are shown in Figure 21 which gives both the initial velocity and the corrected velocity as a function of the angle.

The suppressed velocity distribution shown in Figure 21 was difficult to approximate analytically. Hence the integration of Eq. (5) was carried out numerically, using Eq. (7) for an arbitrary normalization to 100. Figure 22 shows the decay distribution curves computed for the idealized and perfect one-sided collimator for assumed half-lives of 0, 4, 8, and 12 x 10^{-12} seconds.

C. Results and Discussion

Table III lists the half-life values determined by comparing the experimental decay distribution curves with the curves computed as described in Section B. (As noted earlier one such comparison is illustrated in Figure 23.)

TABLE III

Measured Half-Life Values

Number of run group	$t_{1/2}$ (in 10^{-12} seconds)	Relative weight on basis of number of points taken
1	3	7
2	11	14
3	5	16
4	12	18

The overall mean value of the half-life, weighted as indicated, is 8.6×10^{-12} seconds, where the standard deviation of the above values is 3.6×10^{-12} seconds. However, because of the approximations in the construction of the theoretical recoil decay distributions, resulting primarily from uncertainties in the range-velocity relation for the O^{16} ions, and the uncertainty in the determination of the best fits of the folded distributions to the observed distributions, the probable error will be quoted as 4.0×10^{-12} seconds.

A further source of uncertainty in the analysis arises from the ambiguity in the choice of the relative amplitude and phase, $Be^{i\beta}$, for the outgoing d- and g-wave α particles. A measure of the effect of the various suggested values of B and $\cos\beta$ is given in the following table, where $N_{-}(0,\infty)$ is the relative number of

γ rays emitted perpendicular to the beam direction from nuclei recoiling in the backward hemisphere (N_{total} = 100.0), and $\bar{v}_z$ is the mean z component of velocity in the backward direction of these recoils.

TABLE IV

Effect of the relative amplitude and phase, $Be^{i\beta}$, of the outgoing d- and g-wave α particles on $N_-(0,\infty)$, the number of γ rays emitted perpendicular to the beam direction from nuclei recoiling into the backward hemisphere, and on $\bar{v}_z$ the mean z component of velocity of these recoils.

B	$\cos\beta$	$N_-(0,\infty)$(in %)	$\bar{v}_z$ (in 10^8 cm/sec)	$\bar{v}_z N_-$
0.85	+0.242	16.8	0.62	10.4
0.54	-0.245	16.7	0.63	10.5
0.20	-0.242	15.4	0.59	9.1

The product, $\bar{v}_z N_-(0,\infty)$, gives a crude estimate of the relative positions of the centroids of the theoretical decay distributions for the various choices of $Be^{i\beta}$. Compared to other sources of error in the experiment it would appear that this ambiguity should not be regarded as very serious.

A source of error not considered so far is a possible blistering of the covering layer of copper due to heating during bombardment. This effect would allow the recoils to leave the target layer to some extent. After the runs were completed, the target spots were examined visually under a microscope and they appeared to be free

of such effects at the time of inspection. This does not completely eliminate the possibility of the blistering appearing only during the bombardment followed by recovery at its termination, but it seems unlikely that such blistering would disappear without any trace. Another possible effect having to do with the target structure was indicated by the noticeable decline in counting rate as the bombardment continued. This may have been due to loss of fluorine from the target layer which would therefore be changing in effective composition. This could well give rise to a somewhat different energy loss for the escaping O^{16*} recoils than was actually allowed for in the analysis. Temperature changes in the various parts of the mechanism could cause changes in the relative positions of the target and collimator during a run. Temperatures were not monitored; however, because of the large cross section of the shaft it is difficult to see how any significant differences could be maintained along the shaft. Effects due to overall temperature changes were also believed to be insignificant because to a reasonable approximation the thermal expansion of the shaft supporting the target was in turn compensated by a corresponding expansion of the shaft positioning parts. The overall shift of one run relative to another sometimes seen, as noted already, might have been due, at least in part, to a slight realignment of the shaft in its supporting cylinder which occurred during the resetting of the target position preceding each run. Such effects were not believed serious because it was consistently observed that the shapes of the curves were in good correspondence, i.e. the unexplained shifts did not occur during a run, which involved only a slight turning of the bronze nut for each successive point, but

rather between runs when the nut was completely repositioned, amounting to about 10 full revolutions. The evaporation of the metallic recoil stopping layer which took place between the recoil and no-recoil runs involved a considerable, though temporary, increase in temperature. This might have introduced some of the shift between the recoil and no recoil groups through a redistribution of the lubricating layer in the threads of the differential screw. A thinning of the lubricating layer occurring between the two groups of runs would have been consistent with the observed direction of the shift. Again this was not very serious because the experiment required an analysis only of the relative shapes of the curves.

Some possible means of improving the accuracy of and the lower limit of lifetime attainable by the recoil technique should be pointed out. The collimator lead blocks could be moved closer together, provided that the reaction under study had sufficient yield. A factor of two reduction in the separation of the blocks would steepen the slope of the transmission curve by a factor of two near the top of the edge, and would give a relatively much larger difference in transmission at the toe of the curve. This would then provide a much greater distinction in the shapes of the curves given by the recoil and no recoil runs. In addition, it would be desirable to make some arrangement, perhaps optical, to measure independently the relative separation of the target and collimator rather than to use only the setting of the differential screw to determine this quantity.

Other critical features of the technique are the target flatness and parallelism with the collimator, beam position relative

to the collimator, target thickness, and carbon deposition on the target. With the suggested changes in the collimator and position measuring system, and with careful attention to the above noted critical items, it should be possible to reduce the uncertainty in measurement of lifetimes of this order of magnitude by a factor of two or three. Accordingly this would allow the measurement of correspondingly shorter lifetimes.

D. Comparison of the Observed Mean Life with Various Theoretical Estimates for the 6.14-Mev State

The single-particle limit for the mean life of this state, as given by the Weisskopf formula for γ ray transition rates (1), is 2.1×10^{-10} seconds, where the radius of the O^{16} nucleus has been taken to be $1.30 \times (16)^{1/3} \times 10^{-13}$ cm, in agreement with the indications of recent electron scattering experiments with light nuclei (26, 27, 28). The measured value, $(1.2 \pm 0.6) \times 10^{-11}$ seconds, is shorter than this estimate by a factor of about 17 and hence indicates very strongly that this transition is not of a single-particle nature.

The α-particle model for the O^{16} nucleus has been worked out in considerable detail by Kameny (29). He gives an estimate of 3.2×10^{-11} seconds for the 6.14-Mev state lifetime using α-particle wave functions which had already been adjusted to give a reasonable fit to the known O^{16} level scheme. The experimental lifetime is still somewhat shorter than this value and indicates that, while the static properties of the O^{16} states of O^{16} can be accounted for fairly well by α-particle model wave functions, the dynamical aspects of these wave functions may still be in error. This conclusion is supported by a comparison of Kameny's calculations (29) of the transition rates for the low lying O^{16} states and the corresponding experimental values for these rates.

Shell model estimates of the lifetime have been about an order of magnitude too long. Elliot and Flowers give a value of 1.2×10^{-10} seconds, based on their shell model calculations (30). This result and a similar result by R. A. Ferrell (31) indicate that the shell model wave functions, as developed so far, still do not

give a sufficiently detailed description of the O^{16} ground state and 6.14-Mev excited state.

In view of the apparent difficulty in finding nuclear wave functions which will give this very fast transition rate Ferrell (31) and Lane (32) have calculated the maximum possible value which could be obtained with a strict shell model ground state wave function (doubly closed shells of completely uncorrelated individual nucleons) and the most general possible wave function for the excited state. The E3 operator was applied to the above ground state to generate directly that specially constructed excited state wave function which would have the maximum possible E3 transition rate to the assumed ground state. One half of this sum rule limit represents transitions to all the $T = 0$ excited states, including the 6.14-Mev $T = 0$ state, and results in a corresponding lower limit of about 2.2×10^{-11} seconds for the mean life. The above limit, which results from the use of pure oscillator wave functions a $(1s)^2 (1p)^6$ proton configuration and nuclear sizes determined from the electron scattering studies (26, 27, 28) at Stanford University in the evaluation of the required matrix element of r^6, is in disagreement with the measured value by roughly a factor of two. This rule unrealistically assumes no nucleon-nucleon correlations and hence any such disagreement is not at all unreasonable. However, in addition a more general ground state wave function can be considered (31, 32) by using another electric octupole sum rule which can be derived, for instance, in the same manner as was done for an electric monopole sum rule (33). That sum rule makes it possible to calculate the maximum possible E3 transition rate independently of any assumptions as to the correlations

of the nucleons in the O^{16} ground state as well as in the excited state. This maximum possible transition rate computed, as before, for the $T = 0$ to $T = 0$ transitions and with the use of the same ground state wave function in the evaluation of the required matrix element of r^4, corresponds essentially to an absolute lower limit of about 3.8×10^{-12} seconds for the mean life. Ferrell (31) has also pointed out that if one were to use some exponential tail in the radial wave functions, these limits would be further decreased, perhaps even enough to remove the discrepancy noted with the first considered sum rule.

Hence, while the various nuclear models noted above all give lifetimes rather longer than the observed value, there seem to exist possible wave functions for the two states involved which would have an E3 matrix element between them large enough to give the observed short lifetime. From the second sum rule, and the fact that the next 3^- state (very probably a $T = 1$ state anyway) seems to be at about 12 Mev, it appears that the E3 width to the 6.14-Mev state must represent at least one half of the total E3 width of the O^{16} ground state to all $T = 0$ excited states of O^{16}.

A further and more detailed discussion of the two sum rules used in this section appears in an Addendum, pages 85 - 88.

APPENDIX I.

The Relationship of γ-Ray Lifetime to Doppler Shift, Slowing-Down Time, and dE/dx

The mean Doppler shift in energy of a γ ray emitted from a nucleus produced in an excited state at $t = 0$ and moving thereafter with a velocity $v(t)$ is given, to a good approximation for $\frac{v}{c} << 1$, by

$$\Delta E_\gamma = E_\gamma^o \cos\theta \int_o^\infty \frac{e^{-t/\tau}}{\tau} \frac{v(t)}{c} dt. \qquad AI(1)$$

Here θ is the angle of emission of the γ ray (in the laboratory system) relative to the direction of v and E_γ^o and τ are respectively the center of mass γ-ray energy and the mean life of the γ-ray emitting state.

An approximate relation, for ions of velocity in the range of a few times 10^8 cm/sec., between their residual range, R, and velocity, v, is given by

$$R = \alpha v. \qquad AI(2)$$

Using this, one has immediately $\frac{dR}{dt} = -v = \alpha \frac{dv}{dt}$ and hence it follows that

$$v(t) = v_o e^{-t/\alpha} . \qquad AI(3)$$

With this form substituted for $v(t)$ in eq. AI(1) the integration results in

$$\Delta E_\gamma = E_\gamma^o \cos\theta \int_o^\infty \frac{e^{-\frac{\tau+\alpha}{\tau\alpha}t}}{\tau} \frac{v_o}{c} dt = \Delta E_\gamma^{max} \cos\theta \frac{\alpha}{\tau+\alpha} , \qquad AI(4)$$

where ΔE_γ^{max} ($\equiv \frac{v_o}{c} E_\gamma^o$) is the maximum Doppler shift that could occur. One could now measure E_γ at two different values of cos θ and then determine the ratio

$$\frac{\Delta E_\gamma^{obs}}{\Delta E_\gamma^{max} (\cos \theta_2 - \cos \theta_1)} = \frac{\alpha}{\tau + \alpha} \qquad \text{AI(5)}$$

from which, given α, the mean life, τ, can be found.

Alternatively cos θ could be held fixed and a difference in Doppler shifts then measured for recoils traveling alternately into two different media of slowing down times, α_1 and α_2, say. Then the following relation is found:

$$\frac{\Delta E_\gamma^{obs}}{\Delta E_\gamma^{max} \cos \theta} = \frac{\alpha_2}{\tau + \alpha_2} - \frac{\alpha_1}{\tau + \alpha_1} \qquad \text{AI(6)}$$

which, for the often occurring situation where one of the media is simply vacuum (with α_2, say, = ∞) reduces to the particularly simple form

$$\frac{\Delta E_\gamma^{obs}}{\Delta E_\gamma^{max} \cos \theta} = 1 - \frac{\alpha_1}{\tau + \alpha_1} = \frac{\tau}{\tau + \alpha_1} \quad . \qquad \text{AI(7)}$$

This latter situation is the one that corresponds to the experimental arrangement employed in this research to study the lifetime of the first excited state of Be^{10}.

In the event that the lifetime is short compared to the slowing down time, as appears to be the case in the Be^{10} experiment, essentially the same relationship, AI(7), can be shown to exist even without the assumption, $R = \alpha v$. Note that if one lets $R = f(v)$, then in the neighborhood of $v = v_o$, the range-velocity relationship

can be represented by

$$R = \alpha v + R_o, \qquad \text{AI(8)}$$

where $\alpha = \left.\frac{df(v)}{dv}\right|_{v=v_o}$ and R_o is a constant. This in turn results again in AI(3) and hence in AI(4) to AI(7), the latter relations becoming exact in the limit of very short lifetimes. Thus for such a condition one needs to know only the stopping cross section for the ion being studied at, or in the neighborhood of, its initial velocity.

The relationship between dE/dx ($\equiv \varepsilon$) and α may be established as follows. From $E = \frac{1}{2} Mv^2$ one finds

$$\varepsilon = \frac{dE}{dx} = Mv \frac{dv}{dx} = M \frac{dv}{dt}, \qquad \text{AI(9)}$$

and assuming that $\frac{dv}{dt} = -\frac{v}{\alpha}$ it follows that

$$\varepsilon = -\frac{Mv}{\alpha} \quad \text{or} \quad \alpha(v) = \frac{Mv}{\varepsilon(v)}. \qquad \text{AI(10)}$$

The reader is referred to a paper by Devons (2) for formulae for the case where AI(2) is still assumed and the stopping material consists of two layers of different materials superimposed.

APPENDIX II

The Relation Between Doppler Shift and Centroid Shift of a Spectrum

The Doppler shift of the observed γ-ray spectra can be considered, to a good approximation, to be a linear translation of the pulse height curve. This follows because the pair and pair plus one peaks of the spectrum have the same difference in energy from the full energy peak for both the shifted and unshifted spectra. The Compton edge, for high energy γ rays, also has an energy difference relative to the full energy peak that is almost independent of the Doppler shift of frequency. The Doppler shifted curve is then just the unshifted curve translated by an amount Δx.

If the centroid, x_o', of that part of the spectrum, $N(x)$, which appears within a fixed pulse-size "window" extending from x_1 to x_2 is computed, one has

$$x_o' = \frac{\int_{x_1}^{x_2} x\, N(x)\, dx}{\int_{x_1}^{x_2} N(x)\, dx} . \qquad \text{AII(1)}$$

A similar expression for the centroid, x_o'', of the curve shifted toward increasing x by an amount Δx, is obtained by replacing $N(x)$ by $N(x - \Delta x)$ in the integrals from x_1 to x_2. Correcting the shifted centroid for the contribution of that portion of the curve which moves past the fixed window edges, the following expression is found for Δx:

$$\frac{\int_{x_1}^{x_2} xN(x-\Delta x)\,dx - [x_1N(x_1) - x_2N(x_2)]\Delta x}{\int_{x_1}^{x_2} N(x-\Delta x)\,dx - [N(x_1) - N(x_2)]\Delta x} - \frac{\int_{x_1}^{x_2} xN(x)\,dx}{\int_{x_1}^{x_2} N(x)\,dx}.$$

In writing this relation it has been assumed that variations in $N(x)$ within Δx are small compared to $N(x)$ itself. First reducing the above to an expression linear in Δx one finds

$$x = \frac{\int_{x_1}^{x_2} xN(x-\Delta x)\,dx}{\int_{x_1}^{x_2} N(x-\Delta x)\,dx}$$

$$- \Delta x \left\{ \frac{x_1 N(x_1) - x_2N(x_2)}{\int_{x_1}^{x_2} N(x-\Delta x)\,dx} - [N(x_1)-N(x_2)] \frac{\int_{x_1}^{x_2} xN(x-\Delta x)dx}{\left(\int_{x_1}^{x_2} N(x-\Delta x)dx\right)^2} \right\}$$

$$- \frac{\int_{x_1}^{x_2} xN(x)\,dx}{\int_{x_1}^{x_2} N(x)\,dx}. \qquad \text{AII(3)}$$

Then solving for Δx and using the relation, AII(1), the following results:

$$\Delta x = (x''_o - x'_o)\left\{ 1 + \frac{[x_1N(x_1)-x_2N(x_2)]}{\int_{x_1}^{x_2} N(x-\Delta x)\,dx} - [N(x_1)-N(x_2)] \frac{\int_{x_1}^{x_2} xN(x-\Delta x)dx}{\left(\int_{x_1}^{x_2} N(x-\Delta x)dx\right)^2} \right\}^{-1}.$$

AII(4)

This equation now represents the desired relation of the centroid shift, $(x''_o - x'_o)$, to the linear translation, Δx, of the curve.

The above correction factor which gives the shift of the curve, given the centroid shift, can be quite large when the amplitude of the significant features of the function $N(x)$ are not a large fraction of the function itself within the window used. For the spectra of the Be^{10} 3.37-Mev γ ray found in this experiment, that factor is about 3.0.

APPENDIX III

The (α_1, γ_1) Correlation Function for the $F^{19}(p; \alpha_1, \gamma_1) O^{16*}$ Reaction

The correlation function $U(\Theta_\gamma, \Phi_\gamma; \Theta_\alpha, \Phi_\alpha)\, d\Omega_\gamma\, d\Omega_\alpha$ gives the joint probability, per nuclear de-excitation, of the simultaneous emission of a γ ray into a solid angle of $d\Omega_\gamma$ at Θ_γ, Φ_γ and an α particle into a solid angle $d\Omega_\alpha$ at $\Theta_\alpha, \Phi_\alpha$, where the capital Greek letters refer to the center of mass coordinate system with the proton beam chosen as the z-axis. Furthermore this correlation has the property that if it is integrated over the coordinates of the α particle the γ-ray distribution is obtained, and vice versa.

The reaction used in this experiment was the $F^{19}(p;\alpha_1, \gamma_1)O^{16*}$ reaction at a proton bombarding energy of 873 kev. At this energy a compound nuclear state in Ne^{20} with $J^\pi = 2^-$ is formed by p- and f-wave protons ($\ell = 1,3$; $s = \frac{1}{2}^+$) and $F^{19}(J^\pi = \frac{1}{2}^+)$ (15). The proton and F^{19} spins can combine to form channel spins 0 and 1. Ne^{20} ($J^\pi = 2^-$) then decays into d- and g-wave α particles ($\ell' = 2,4$) and $O^{16*}(J^\pi = 3^-)$ which then emits an electric octupole γ ray.

In the present experiment one is interested in γ rays emitted perpendicularly to the proton beam and for convenience a new z axis (z') is chosen perpendicular to the proton beam and along the γ-ray direction. In this coordinate system the coordinates of the proton are $\Theta'_p = \pi/2$, $\Phi'_p = 0$, and the coordinates of the α particle are Θ'_α, Φ'_α, where Θ'_α is the angle between the α particle and the γ ray and Φ'_α is the angle between the p-γ plane and the

$\alpha-\gamma$ plane. The correlation now may be written as a function only of the α-particle coordinates and is given by:

$$U'(\Theta'_\alpha, \Phi'_\alpha) = \frac{3}{64}\frac{1}{1+B^2} \times \qquad \text{AIII(1)}$$

$$\Big[25 + 46\cos^2\Theta'_\alpha - 55\cos^4\Theta'_\alpha - \cos^2\Phi'_\alpha(24 - 24\cos^4\Theta'_\alpha)$$
$$+ \sqrt{10}\, B\cos\beta \Big\{ 10 - 151\cos^2\Theta'_\alpha + 440\cos^4\Theta'_\alpha - 315\cos^6\Theta'_\alpha$$
$$- \cos^2\Phi'_\alpha(11 - 77\cos^2\Theta'_\alpha + 185\cos^4\Theta'_\alpha - 119\cos^6\Theta'_\alpha)\Big\}$$
$$+ \tfrac{5}{2}B^2\Big\{ 4 + 109\cos^2\Theta'_\alpha - 286\cos^4\Theta'_\alpha + 189\cos^6\Theta'_\alpha$$
$$- \cos^2\Phi'_\alpha(3 - 42\cos^2\Theta'_\alpha + 340\cos^4\Theta'_\alpha - 742\cos^6\Theta'_\alpha + 441\cos^8\Theta'_\alpha)\Big\}\Big] .$$

It has been assumed here that only the p-wave protons contribute significantly and this in turn allows only channel spin 1 to contribute. $Be^{i\beta}$ represents the relative amplitude and phase of the g-wave and d-wave outgoing α particles. This correlation has been normalized so that

$$\int_{4\pi} U'(\Theta'_\alpha, \Phi'_\alpha)\frac{d\Omega'_\alpha}{4\pi} = \frac{74 + 95B^2}{80(1+B^2)}, \qquad \text{AIII(2)}$$

which in turn is equal to $W_\gamma(\Theta_\gamma = \frac{\pi}{2})$, where Θ_γ is the polar angle of the γ ray measured with respect to the proton beam direction. Finally, transforming the z axis back onto the proton beam, and averaging over the aximuthal angle of the α particle in the unprimed system, one is led to Eq.(8).

REFERENCES

(1) V. F. Weisskopf, Phys. Rev. 83, 1073 (1951), and J. M. Blatt and V. F. Weisskopf, Theoretical Nuclear Physics, Wiley, New York (1952), p. 627.

(2) Devons, Manning, and Bunbury, Proc. Phys. Soc. (London) A68, 18 (1955).

(3) C. A. Barnes and J. Thirion, 1955 (private communication).

(4) J. Thirion and V. Telegdi, Phys. Rev. 92, 1253 (1953). This article contains references to earlier lifetime work by the recoil method.

(5) C. A. Barnes, 1955, 1956 (private communication).

(6) J. B. Marion and Gustav Weber, Phys. Rev. 103, 167 (1956). A description of the angular distribution chamber constructed by Marion can be found in the reference.

(7) P. K. Weyl, Phys. Rev. 91, 289 (1953).

(8) W. P. Jesse and J. Sadauskis, Phys. Rev. 78, 1 (1950).

(9) A. B. Lillie, Phys. Rev. 87, 716 (1952).

(10) W. Whaling, The Energy Loss of Charged Particles in Matter, p. 193 in Handbuch der Physik, vol. 34, edited by S. Flügge, Springer (1958).

(11) A compilation of stopping cross sections by Ronald Fuchs and Ward Whaling (unpublished).

(12) W. E. Meyerhof and L. F. Chase, Jr., Phys. Rev. (to be published).

(13) R. Montalbetti, Can. J. of Phys. 30, 660 (1952).

(14) R. Hofstadter, Rev. Modern Phys. 28, 214 (1956).

(15) F. Ajzenberg and T. Lauritsen, Revs. Modern Phys. 27, 77 (1955).

(16) J. Seed and A. P. French, Phys. Rev. 88, 1007 (1951).

(17) J. M. Freeman, Phil. Mag. 41, 1225 (1950).

(18) Chao, Tollestrup, Fowler, and Lauritsen, Phys. Rev. 79, 188 (1956).

(19) Devons, Manning, and Towle, Proc. Phys. Soc. (London) A69, 173 (1956).

(20) C. P. Swann and F. R. Metzger, Phys. Rev. 108, 982 (1957).

(21) J. E. Sanders, Phil. Mag. 43, 630 (1952).

(22) Martin, Fowler, Lauritsen, and Lauritsen, Phys. Rev. 106, 1260 (1957).

(23) Peterson, Fowler, and Lauritsen, Phys. Rev. 96, 1250 (1954).

(24) P.M.S. Blackett and D. S. Lees, Proc. Roy. Soc. (London) A134, 658 (1932).

(25) R.D. Evans, The Atomic Nucleus McGraw-Hill Book Co.,Inc., N.Y. (1955), p. 652.

(26) R. Hofstadter (private communication).

(27) R. Hofstadter, Nuclear and Nucleon Scattering of Electrons, pgs. 275 and 276 in Annual Review of Nuclear Science, vol. 7, edited by J. G. Beckerley, Annual Reviews, Inc. (1957).

(28) Ehrenberg, Hofstadter, Meyer-Berkhout, and Sobottka, Phys. Rev. (to be published).

(29) S. L. Kameny, Phys. Rev. 103, 358 (1956).

(30) J. P. Elliott and B. H. Flowers, Proc. Roy. Soc. (London) A242, 57 (1957).

(31) R. A. Ferrell (private communication).

(32) A. M. Lane (private communcation).

(33) R. A. Ferrell, Phys. Rev. 107, 1631 (1957).

(34) J. M. Blatt and V. F. Weisskopf, Theoretical Nuclear Physics, Wiley, New York (1952), p. 640.

(35) R. G. Sachs and N. Austen, Phys. Rev. 81, 705 (1951).

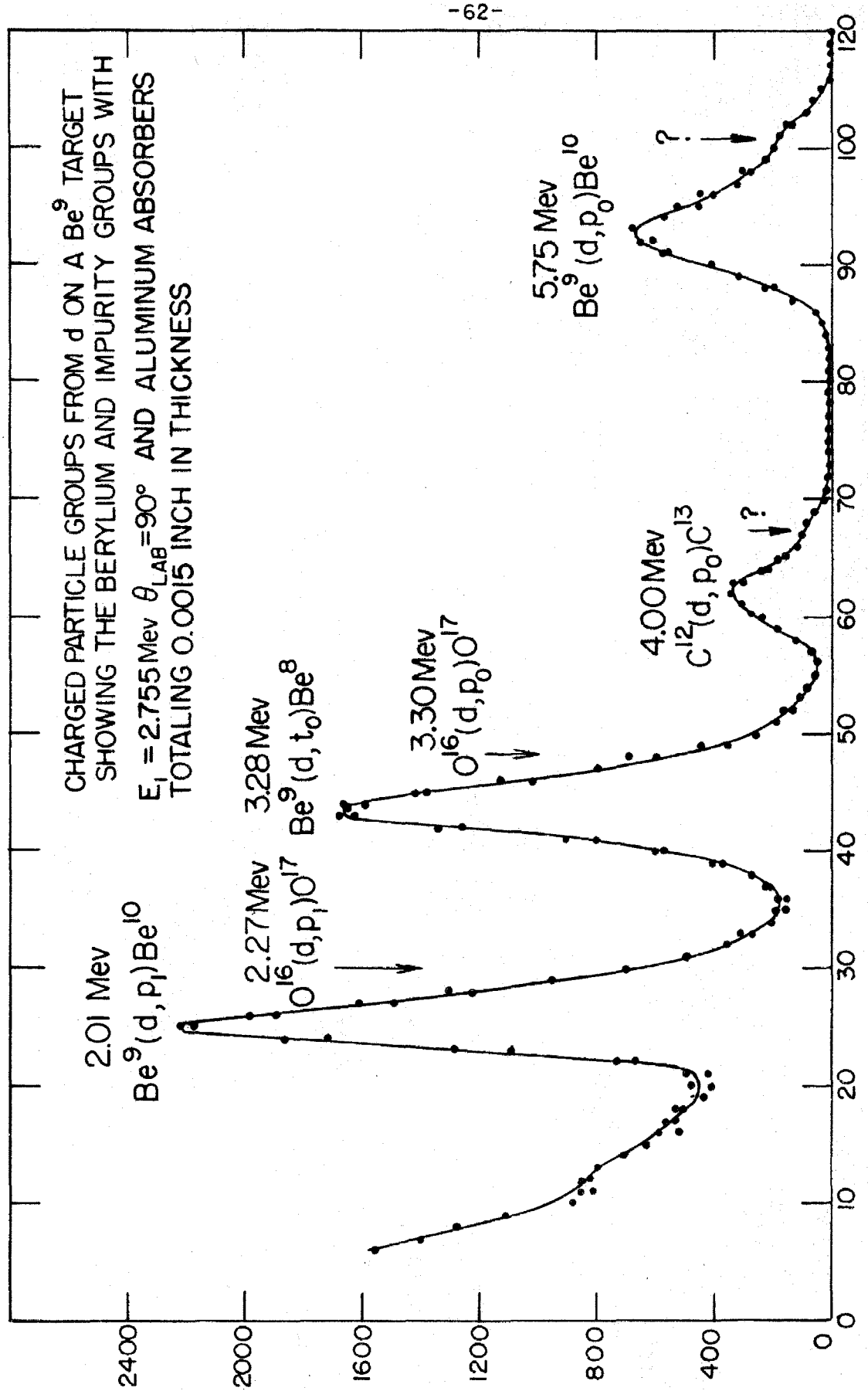
CHARGED PARTICLE GROUPS FROM d ON A Be^9 TARGET
SHOWING THE BERYLIUM AND IMPURITY GROUPS WITH
$E_i = 2.755$ Mev $\theta_{LAB} = 90°$ AND ALUMINUM ABSORBERS
TOTALING 0.0015 INCH IN THICKNESS
2.01 Mev
$Be^9(d,p_1)Be^{10}$
2.27 Mev
$O^{16}(d,p_1)O^{17}$
3.28 Mev
$Be^9(d,t_0)Be^8$
3.30 Mev
$O^{16}(d,p_0)O^{17}$
4.00 Mev
$C^{12}(d,p_0)C^{13}$
?
5.75 Mev
$Be^9(d,p_0)Be^{10}$
?
COUNTS PER CHANNEL PER 15 MICROCOULOMBS
0
400
800
1200
1600
2000
2400
0
10
20
30
40
50
60
70
80
90
100
120
PULSE HEIGHT (VOLTS) (CHANNEL WIDTH = 1 VOLT)

FIGURE 1.

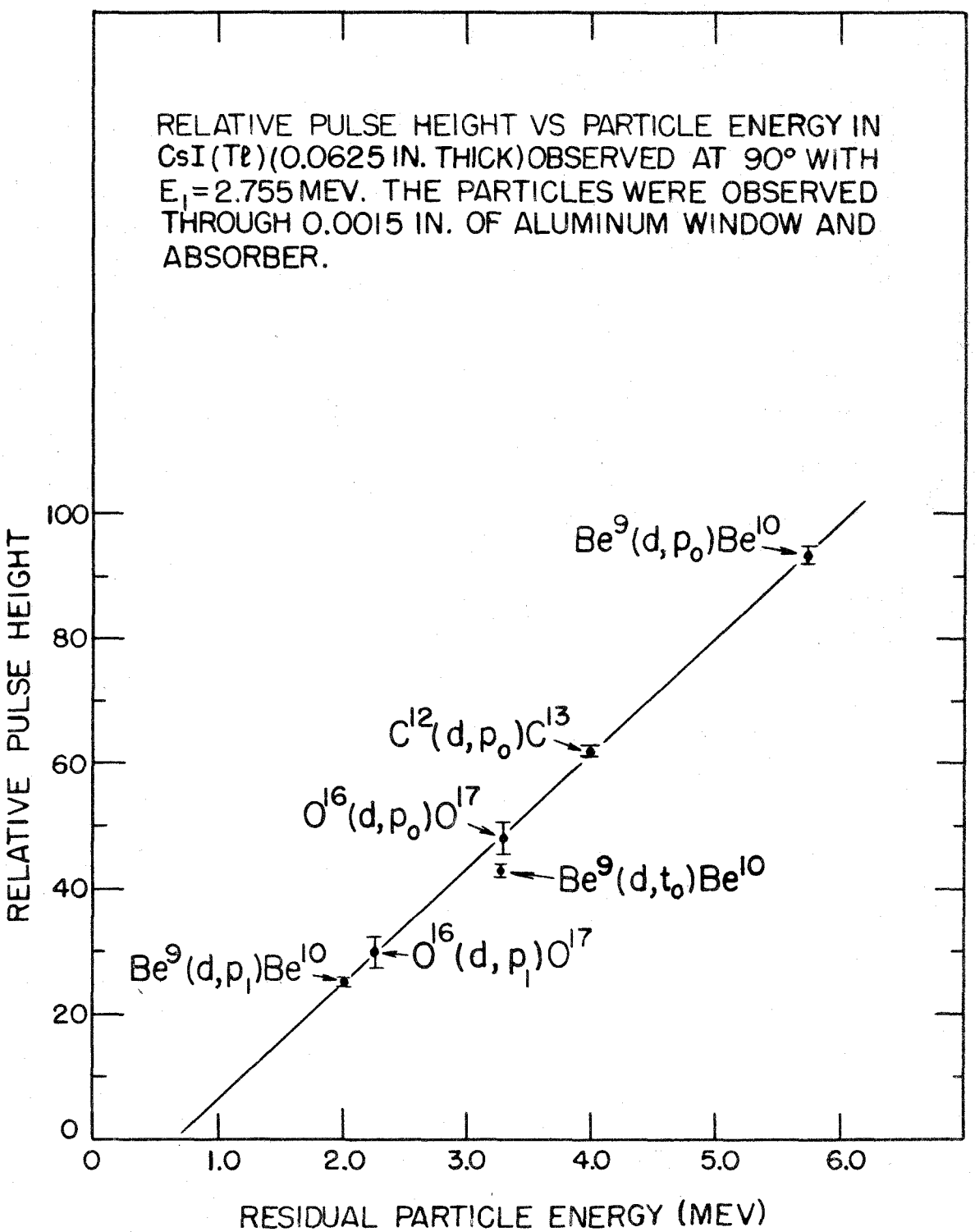
RELATIVE PULSE HEIGHT VS PARTICLE ENERGY IN CsI(Tℓ)(0.0625 IN. THICK)OBSERVED AT 90° WITH E1=2.755 MEV. THE PARTICLES WERE OBSERVED THROUGH 0.0015 IN. OF ALUMINUM WINDOW AND ABSORBER.
RELATIVE PULSE HEIGHT
100
80
60
40
20
0
0
1.0
2.0
3.0
4.0
5.0
6.0
RESIDUAL PARTICLE ENERGY (MEV)
Be9(d,p0)Be10
C12(d,p0)C13
O16(d,p0)O17
Be9(d,t0)Be10
O16(d,p1)O17
Be9(d,p1)Be10

FIGURE 2.

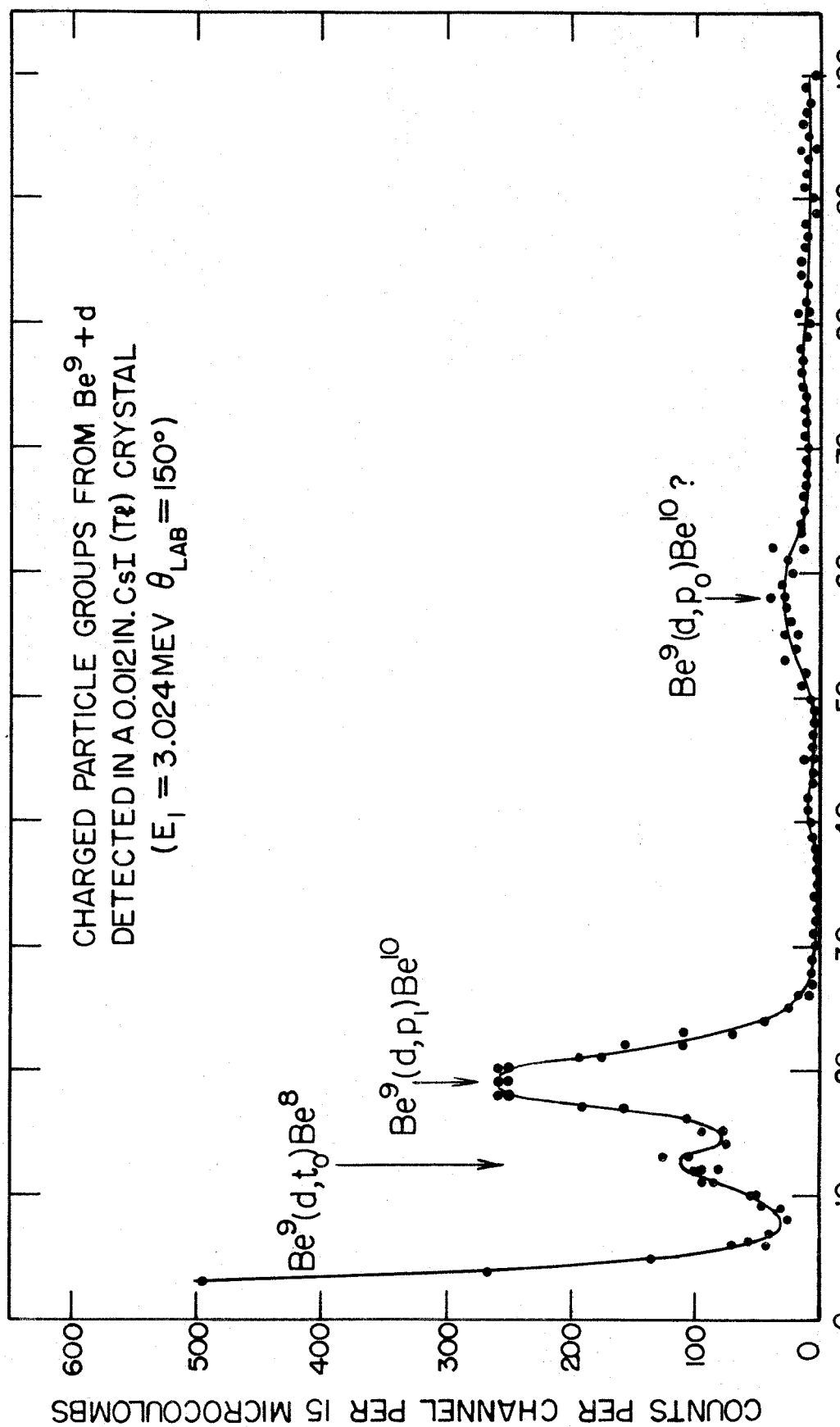
CHARGED PARTICLE GROUPS FROM Be^9 + d
DETECTED IN A 0.012 IN. CsI (Tℓ) CRYSTAL
(E_1 = 3.024 MEV θ_{LAB} = 150°)
$Be^9(d,t_0)Be^8$
$Be^9(d,p_1)Be^{10}$
$Be^9(d,p_0)Be^{10}$?
COUNTS PER CHANNEL PER 15 MICROCOULOMBS
PULSE HEIGHT (VOLTS) (CHANNEL WIDTH = 1 VOLT)
0
100
200
300
400
500
600
10
20
30
40
50
60
70
80
90
100

FIGURE 3.

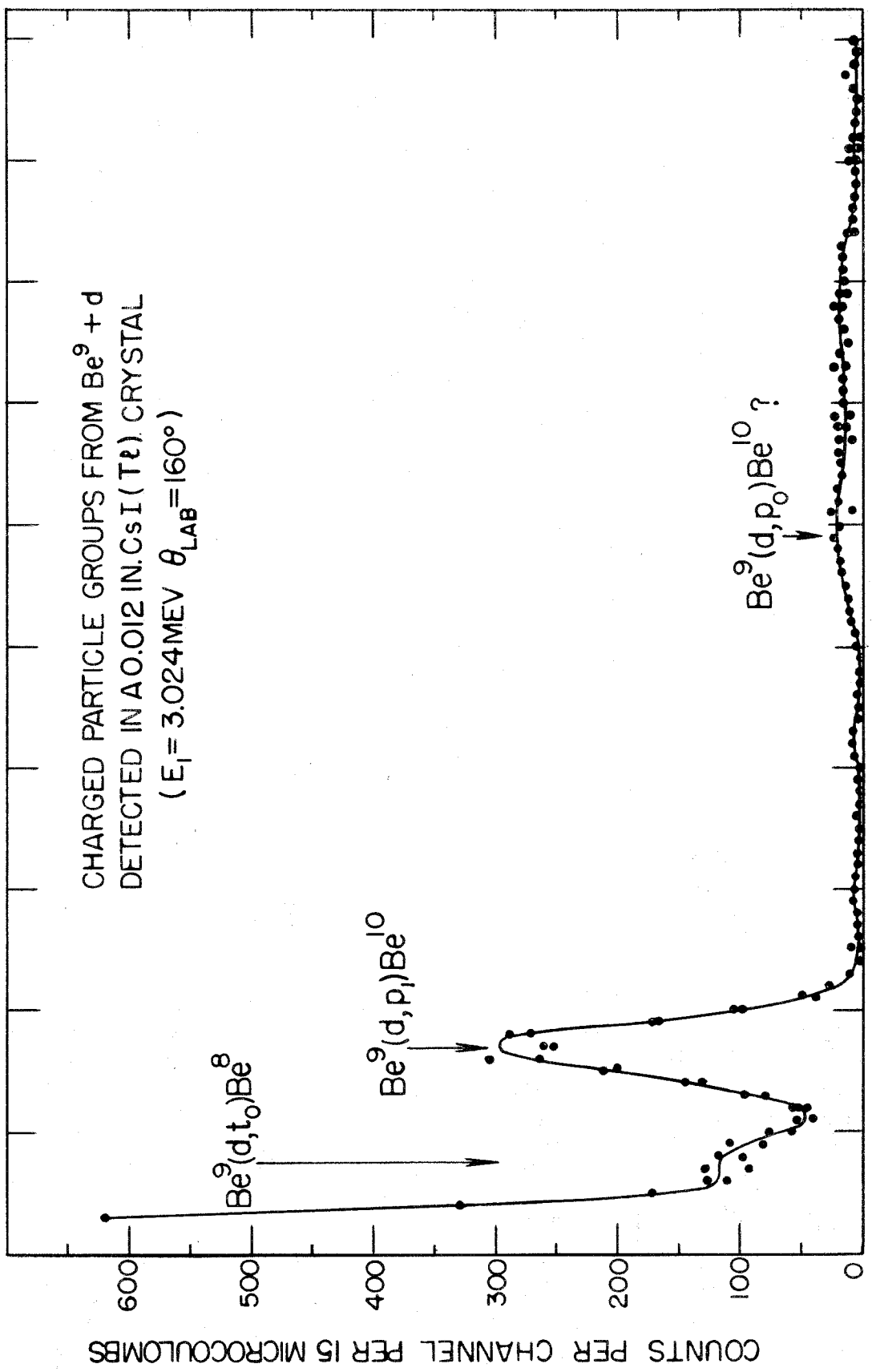
CHARGED PARTICLE GROUPS FROM Be^9 + d
DETECTED IN A 0.012 IN. CsI(Tl) CRYSTAL
(E_I = 3.024 MEV θ_{LAB} = 160°)
$Be^9(d,t_o)Be^8$
$Be^9(d,p_1)Be^{10}$
$Be^9(d,p_o)Be^{10}$?
COUNTS PER CHANNEL PER 15 MICROCOULOMBS
PULSE HEIGHT (VOLTS) (CHANNEL WIDTH = 1 VOLT)
0
100
200
300
400
500
600
10
20
30
40
50
60
70
80
90
100

FIGURE 4.

HORIZONTAL SECTION THROUGH THE TARGET CHAMBER, PROTON DETECTOR, AND γ-RAY DETECTOR ASSEMBLIES

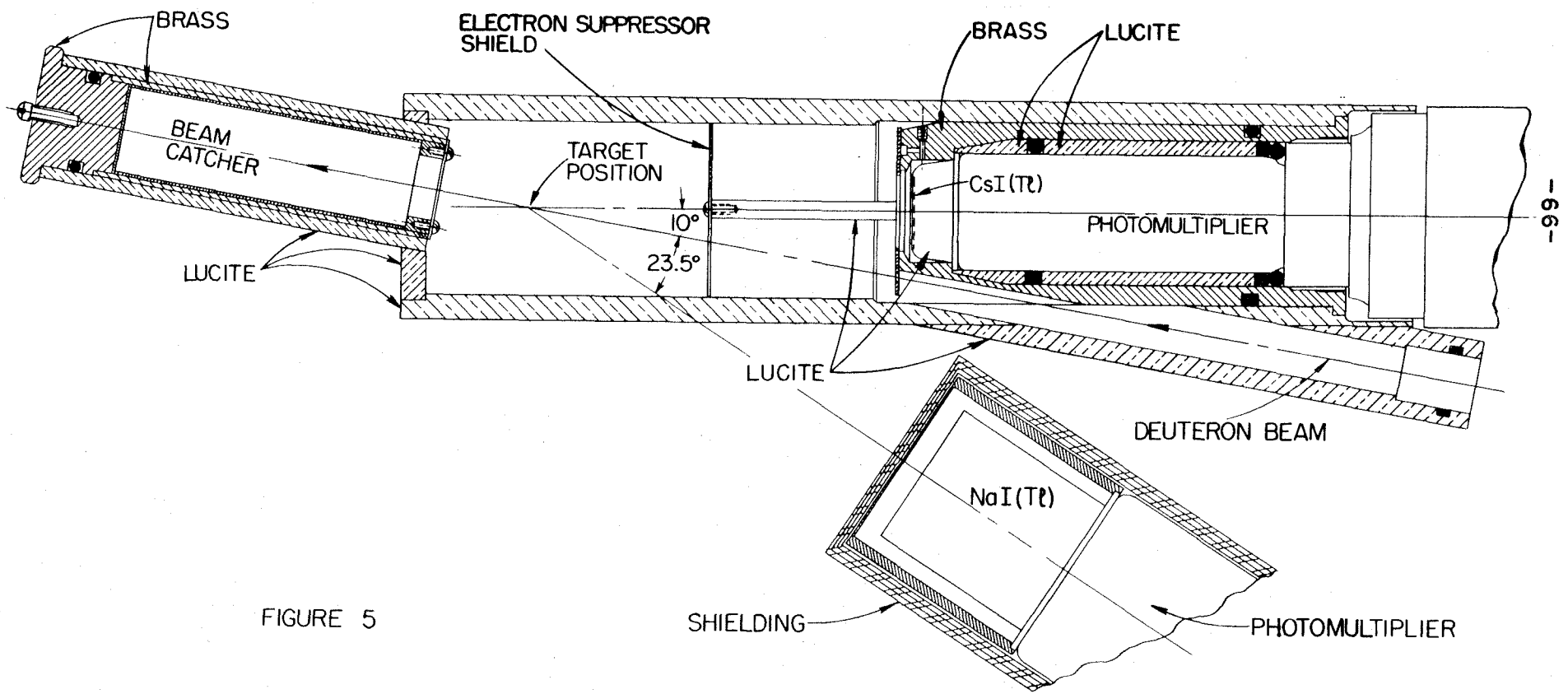

FIGURE 5

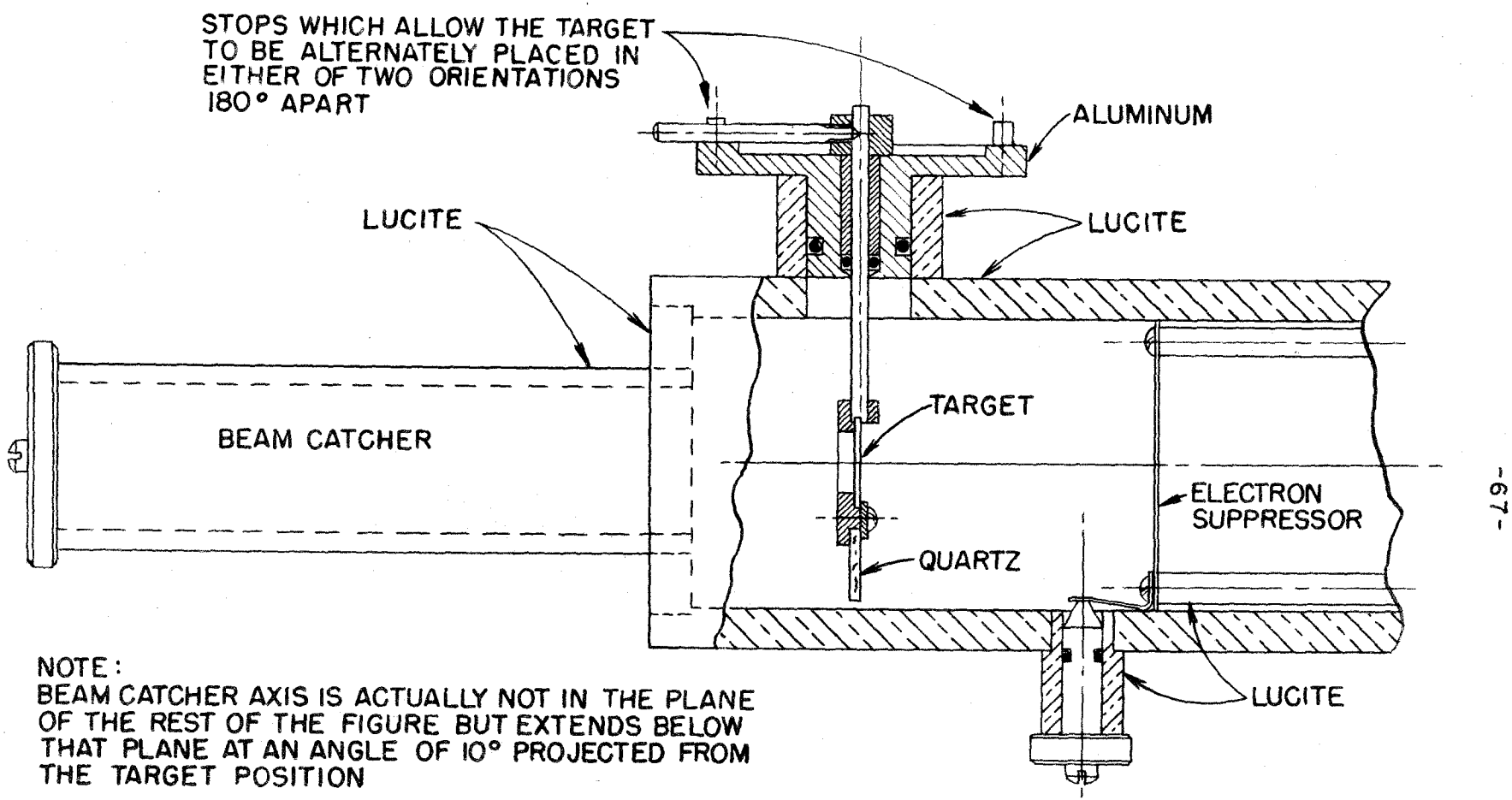

A VERTICAL SECTION THROUGH THE TARGET CHAMBER SHOWING THE TARGET HOLDER ARRANGEMENT

FIGURE 6.

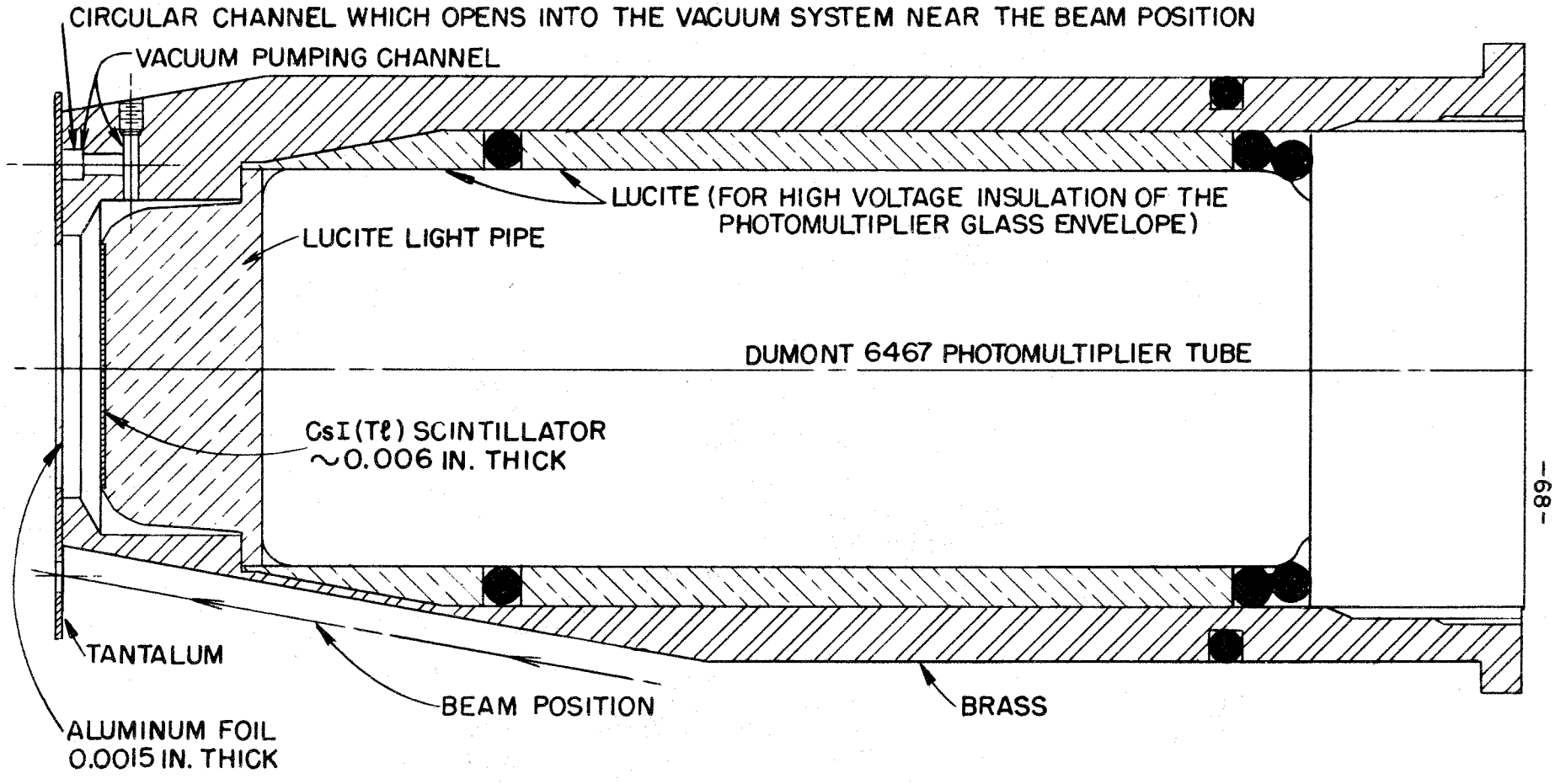

THE PROTON DETECTOR PHOTOMULTIPLIER ASSEMBLY (TWICE FULL SCALE)

FIGURE 7.

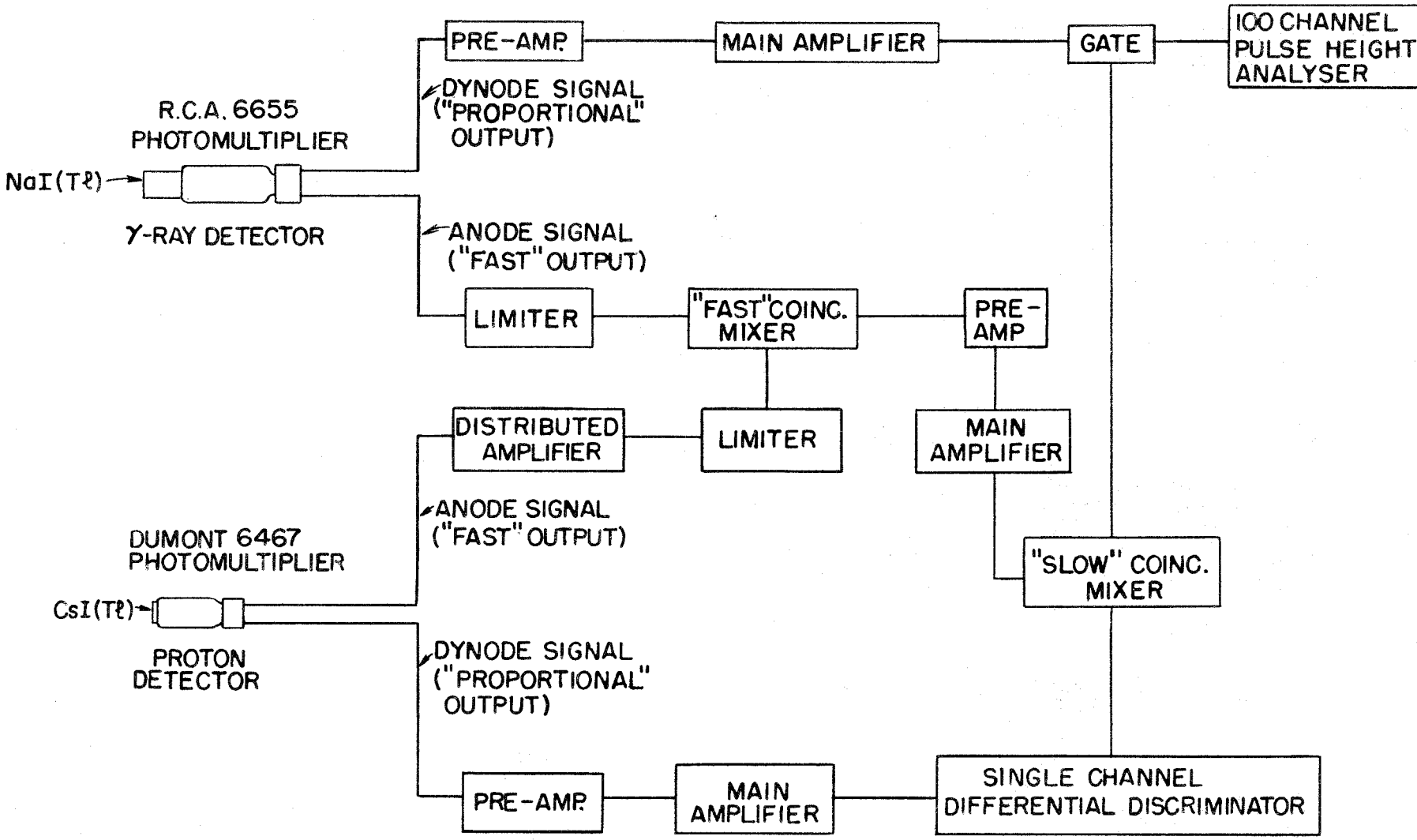

GENERAL SCHEMATIC OUTLINE OF THE ELECTRONIC APPARATUS FOR THE Be^{10} EXPERIMENT

FIGURE 8

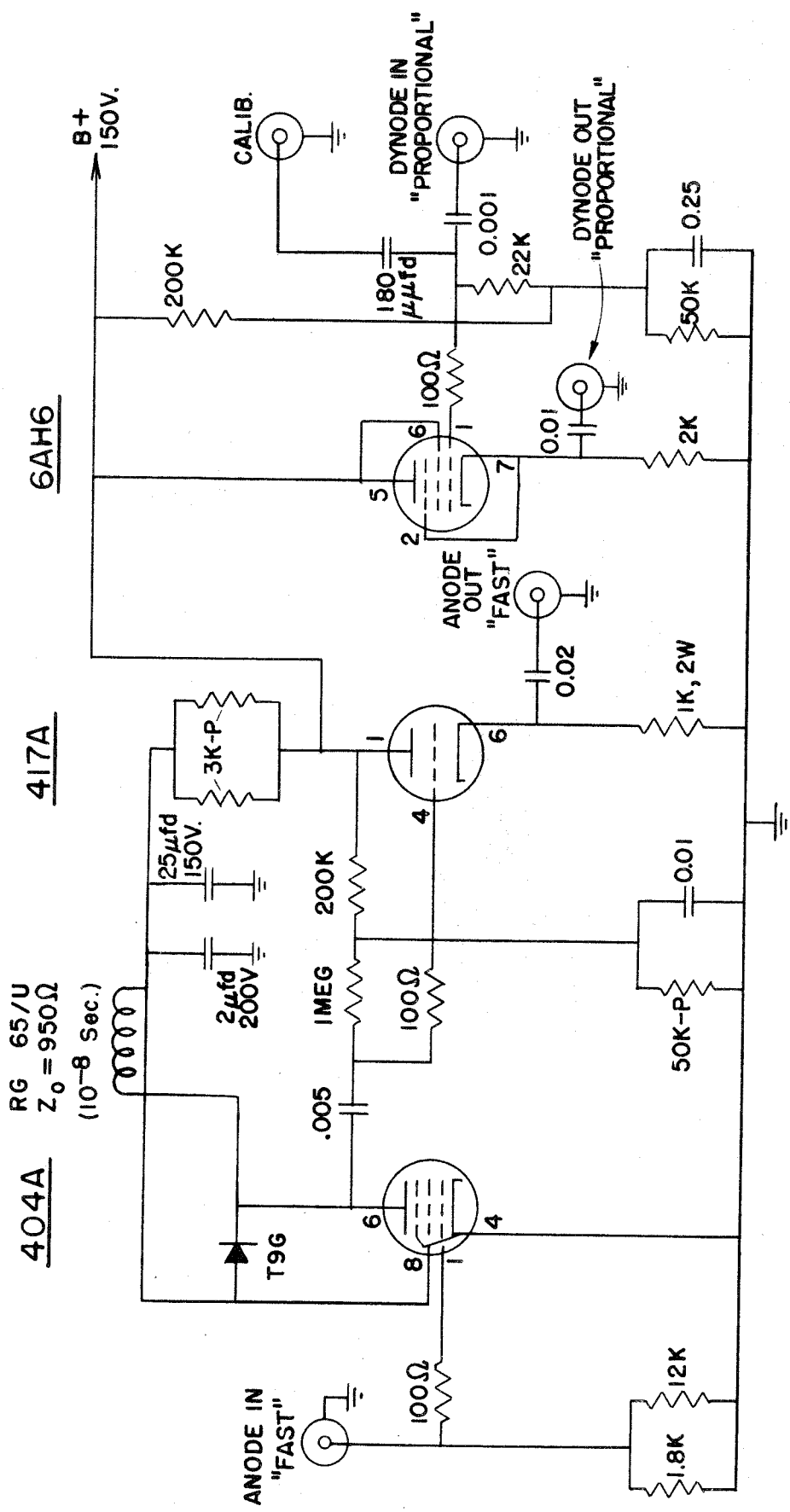

LIMITER AND PRE-AMPLIFIER

FIGURE 9.

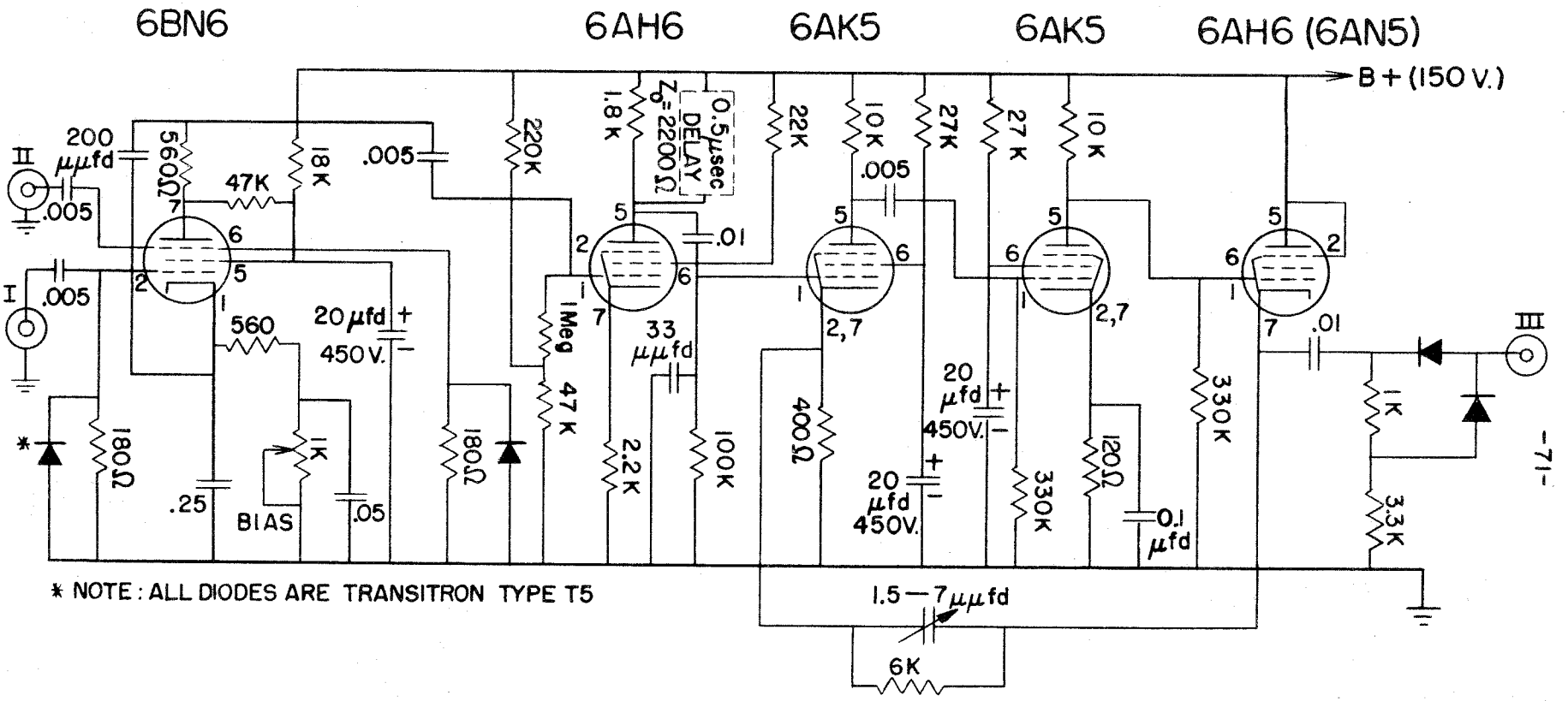

FAST COINCIDENCE MIXER AND PRE-AMPLIFIER UNIT

FIGURE 10.

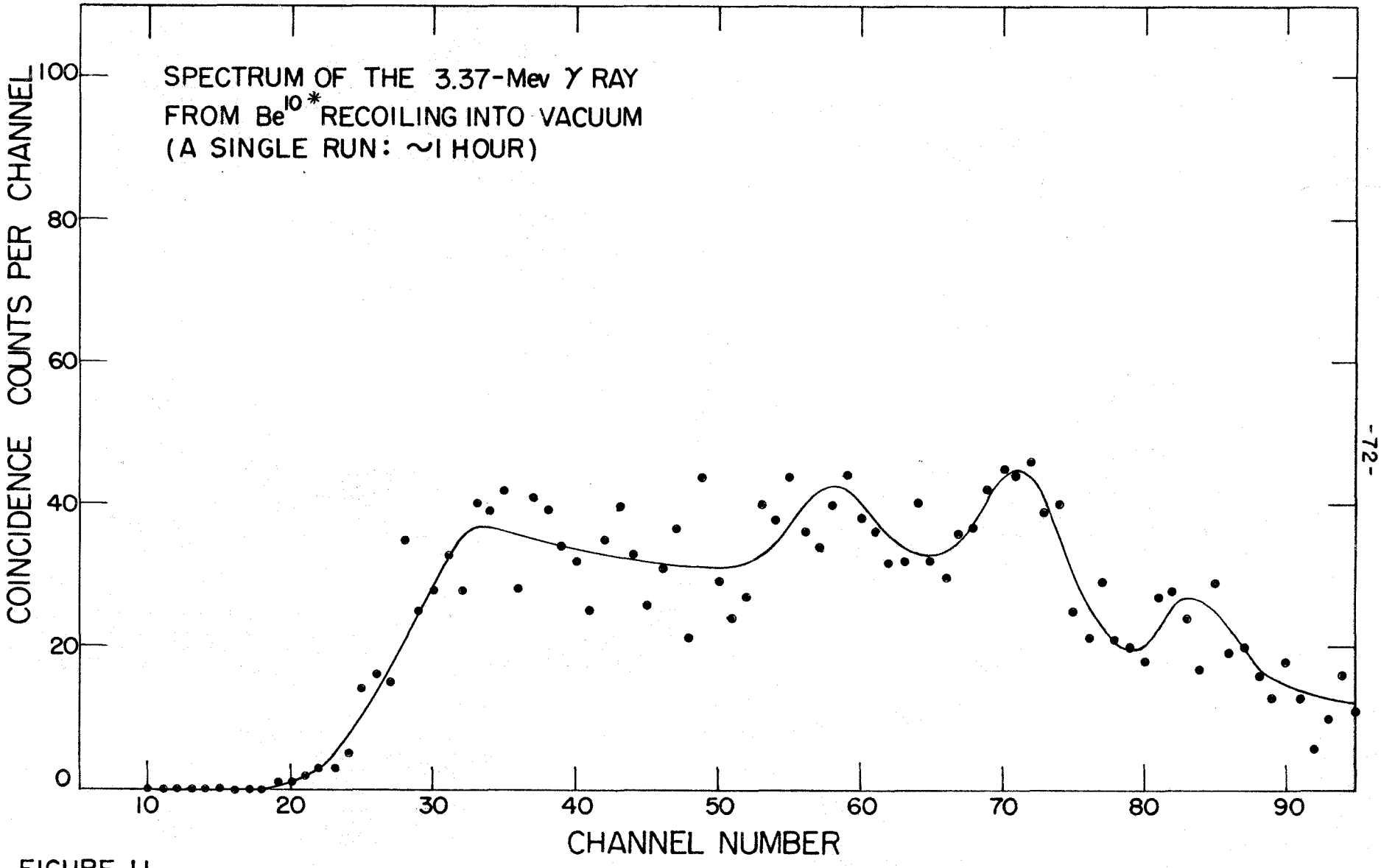
SPECTRUM OF THE 3.37-Mev γ RAY
FROM Be^{10*} RECOILING INTO VACUUM
(A SINGLE RUN: ~1 HOUR)
COINCIDENCE COUNTS PER CHANNEL
0
20
40
60
80
100
10
20
30
40
50
60
70
80
90
CHANNEL NUMBER

FIGURE 11.

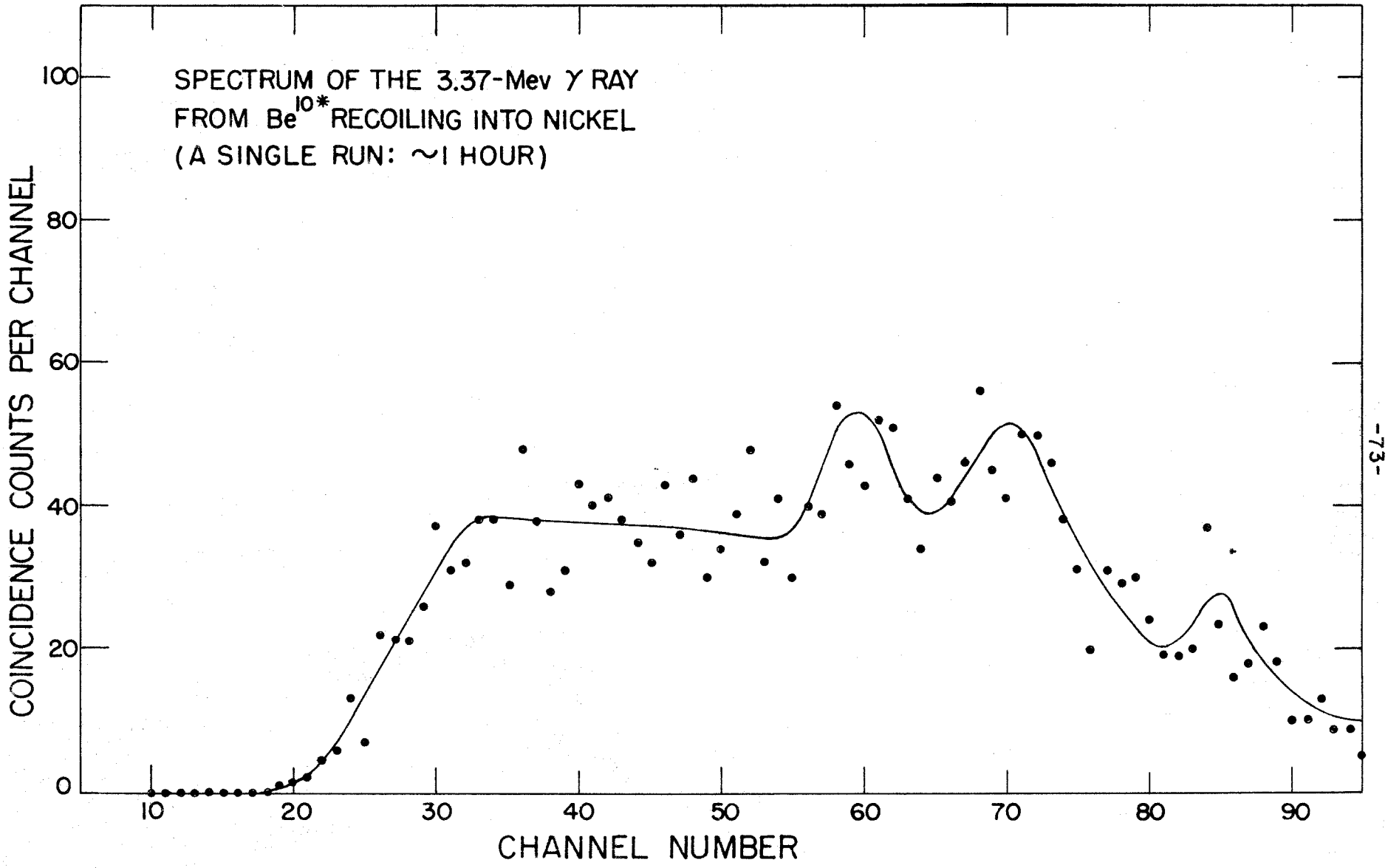
SPECTRUM OF THE 3.37-Mev γ RAY
FROM Be10* RECOILING INTO NICKEL
(A SINGLE RUN: ~1 HOUR)
COINCIDENCE COUNTS PER CHANNEL
CHANNEL NUMBER
0
20
40
60
80
100
10
20
30
40
50
60
70
80
90

FIGURE 12.

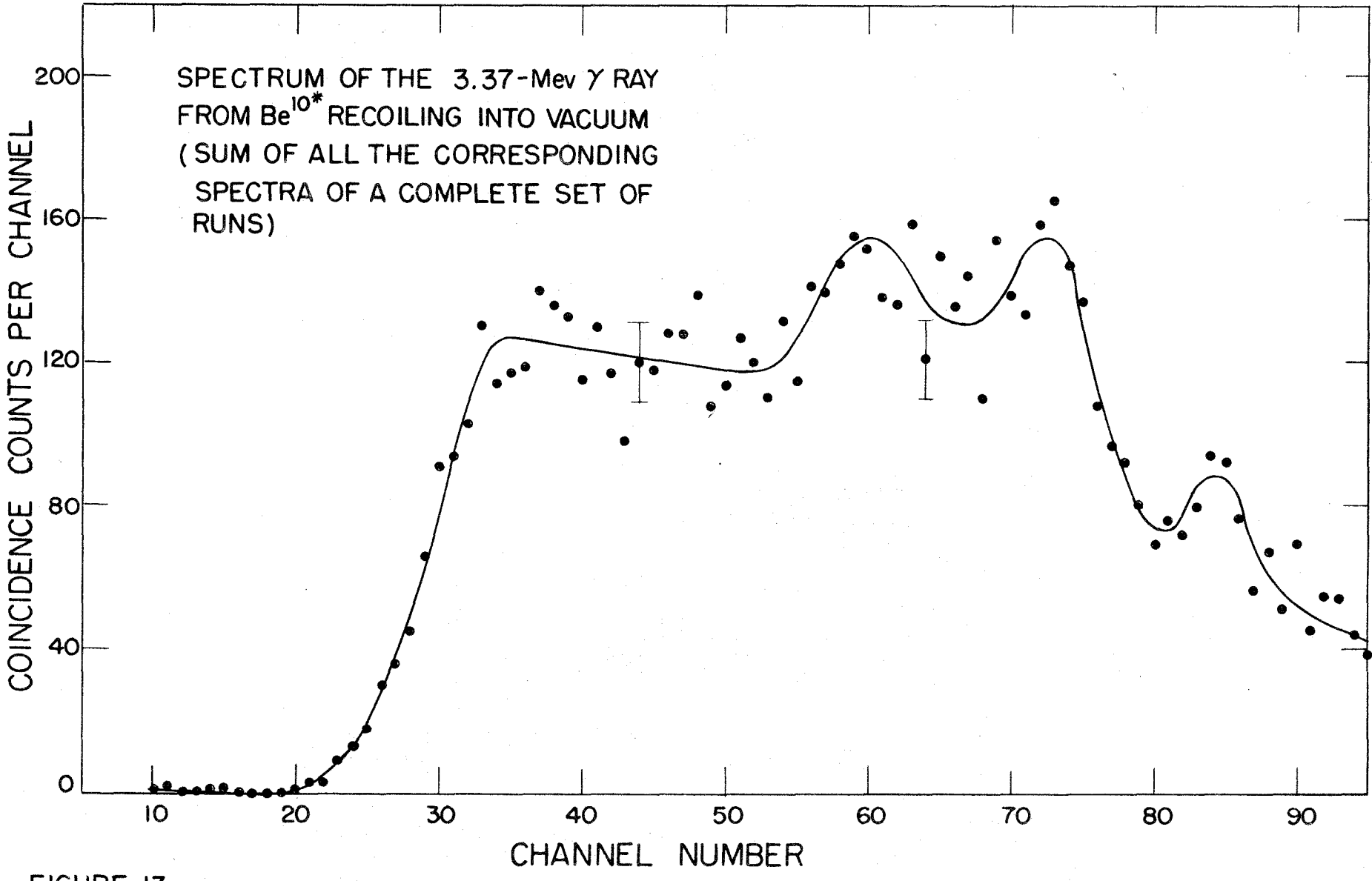
SPECTRUM OF THE 3.37-Mev γ RAY
FROM Be10* RECOILING INTO VACUUM
(SUM OF ALL THE CORRESPONDING
SPECTRA OF A COMPLETE SET OF
RUNS)
COINCIDENCE COUNTS PER CHANNEL
0
40
80
120
160
200
10
20
30
40
50
60
70
80
90
CHANNEL NUMBER

FIGURE 13.

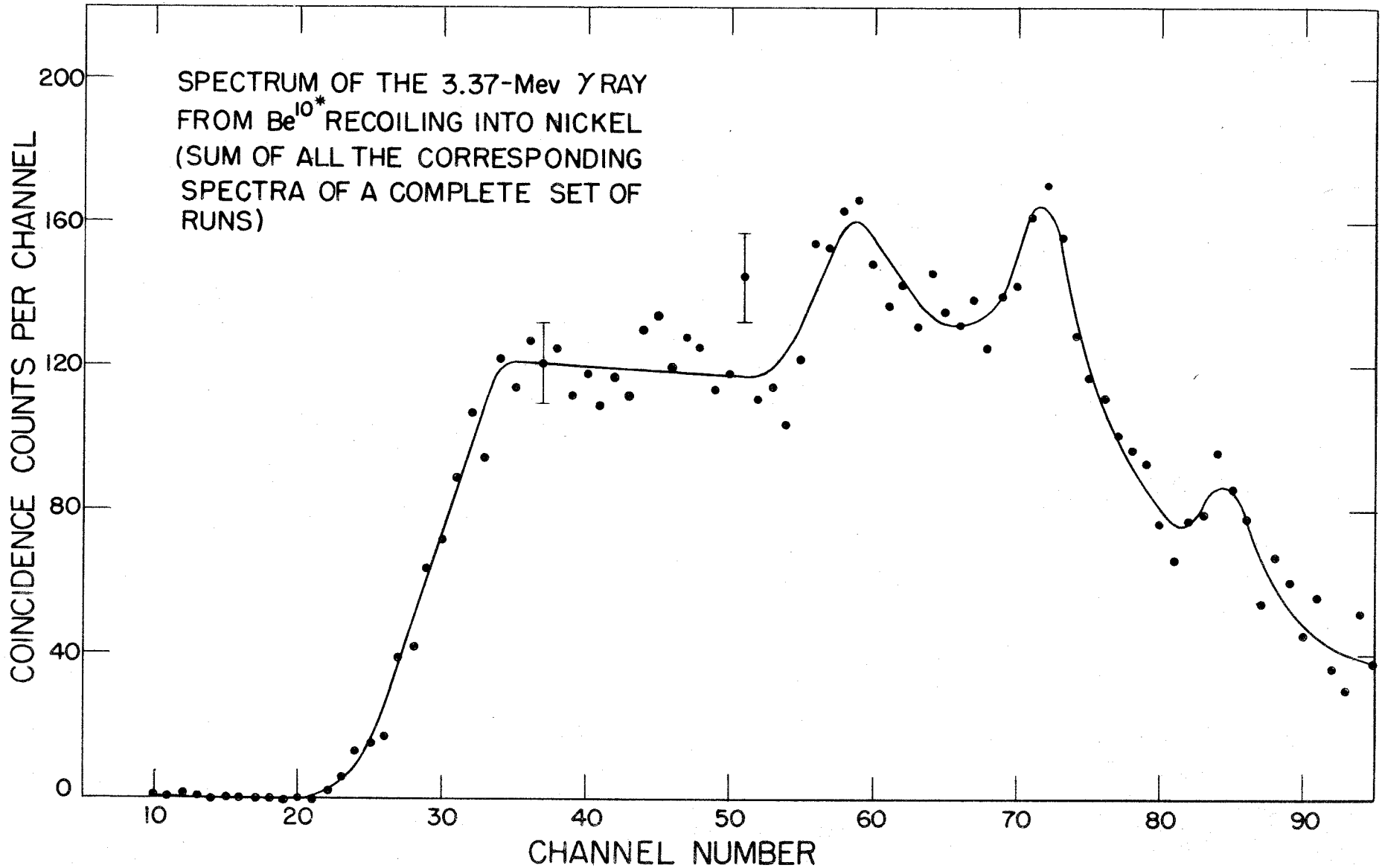
SPECTRUM OF THE 3.37-Mev γ RAY
FROM Be^{10*} RECOILING INTO NICKEL
(SUM OF ALL THE CORRESPONDING
SPECTRA OF A COMPLETE SET OF
RUNS)
COINCIDENCE COUNTS PER CHANNEL
0
40
80
120
160
200
10
20
30
40
50
60
70
80
90
CHANNEL NUMBER

FIGURE 14.

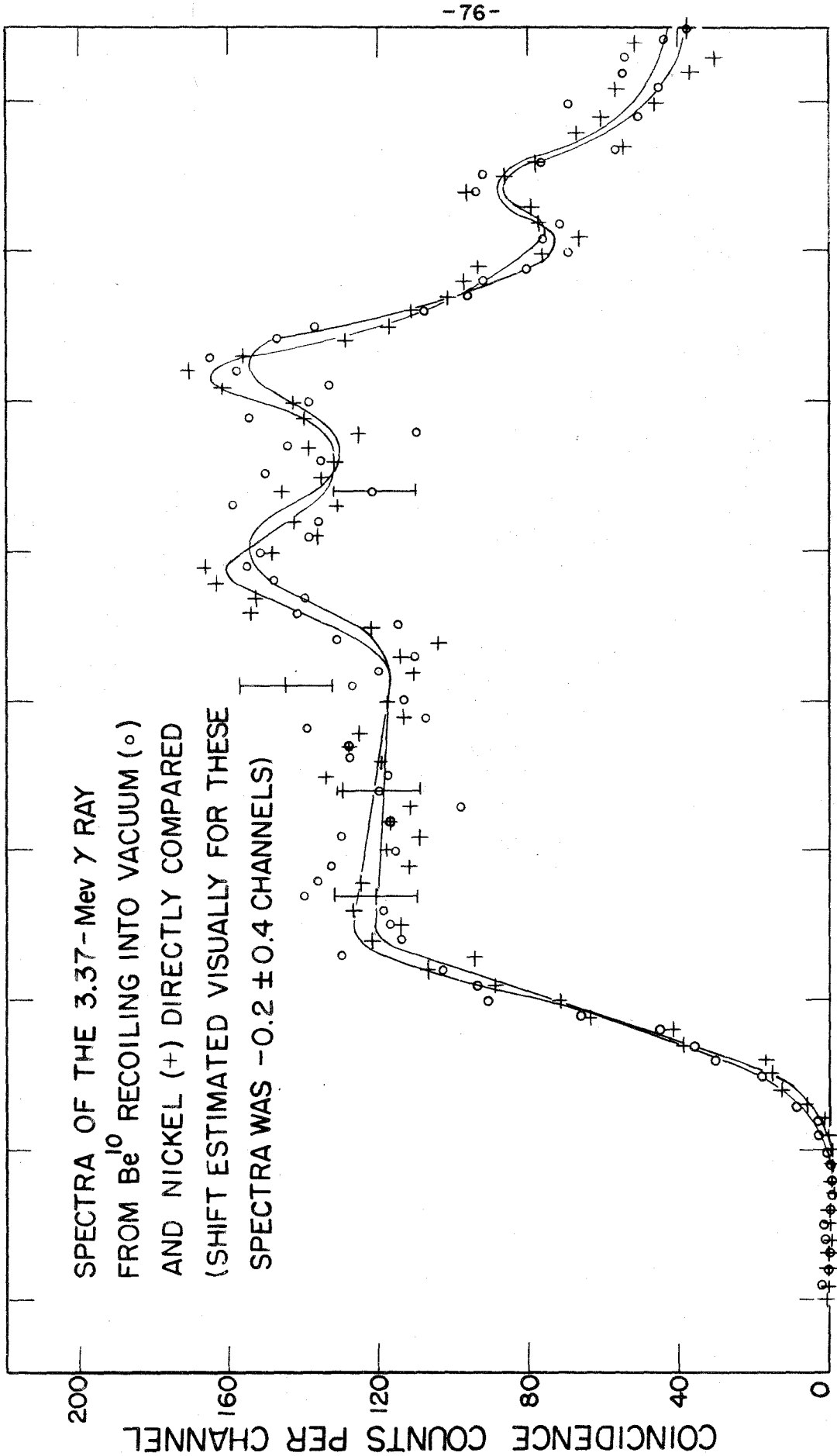
SPECTRA OF THE 3.37-Mev γ RAY
FROM Be^{10} RECOILING INTO VACUUM (○)
AND NICKEL (+) DIRECTLY COMPARED
(SHIFT ESTIMATED VISUALLY FOR THESE
SPECTRA WAS -0.2 ± 0.4 CHANNELS)
COINCIDENCE COUNTS PER CHANNEL
CHANNEL NUMBER
0
40
80
120
160
200
10
20
30
40
50
60
70
80
90

FIGURE 15.

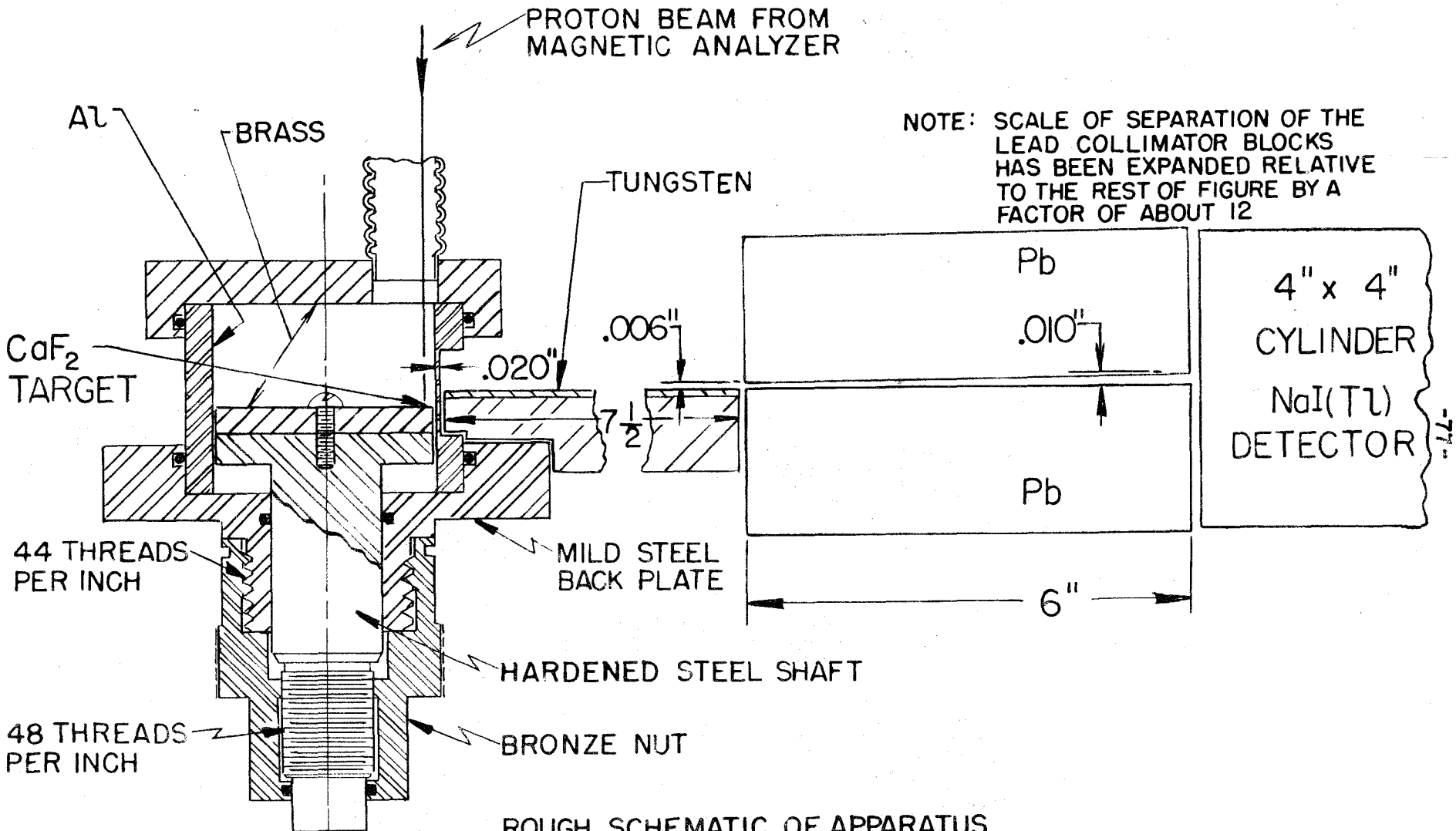

ROUGH SCHEMATIC OF APPARATUS
FOR THE O^{16} 6.14-MEV STATE LIFETIME EXPERIMENT

FIGURE 16.

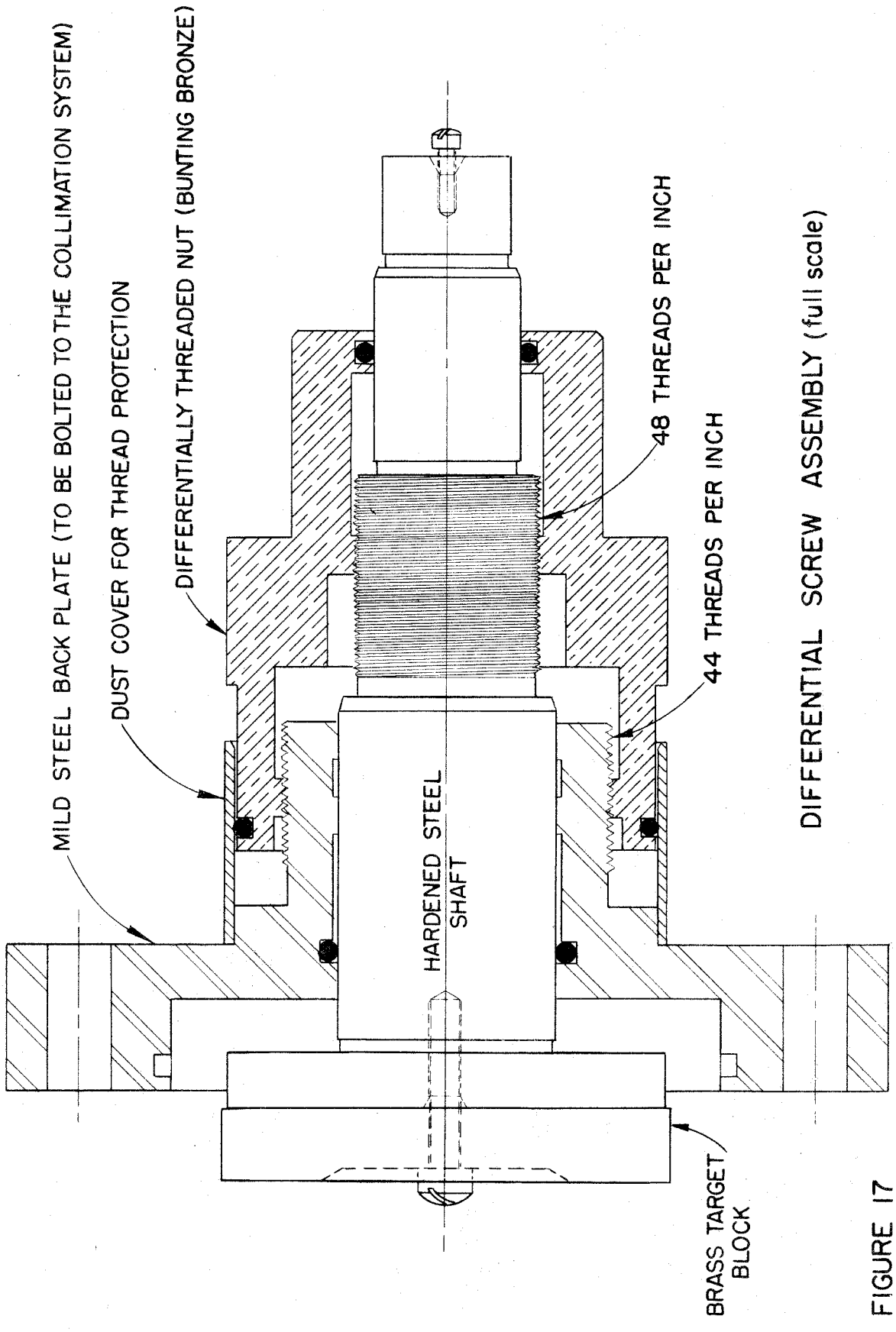
MILD STEEL BACK PLATE (TO BE BOLTED TO THE COLLIMATION SYSTEM)
DUST COVER FOR THREAD PROTECTION
DIFFERENTIALLY THREADED NUT (BUNTING BRONZE)
48 THREADS PER INCH
44 THREADS PER INCH
HARDENED STEEL SHAFT
BRASS TARGET BLOCK
DIFFERENTIAL SCREW ASSEMBLY (full scale)

FIGURE 17

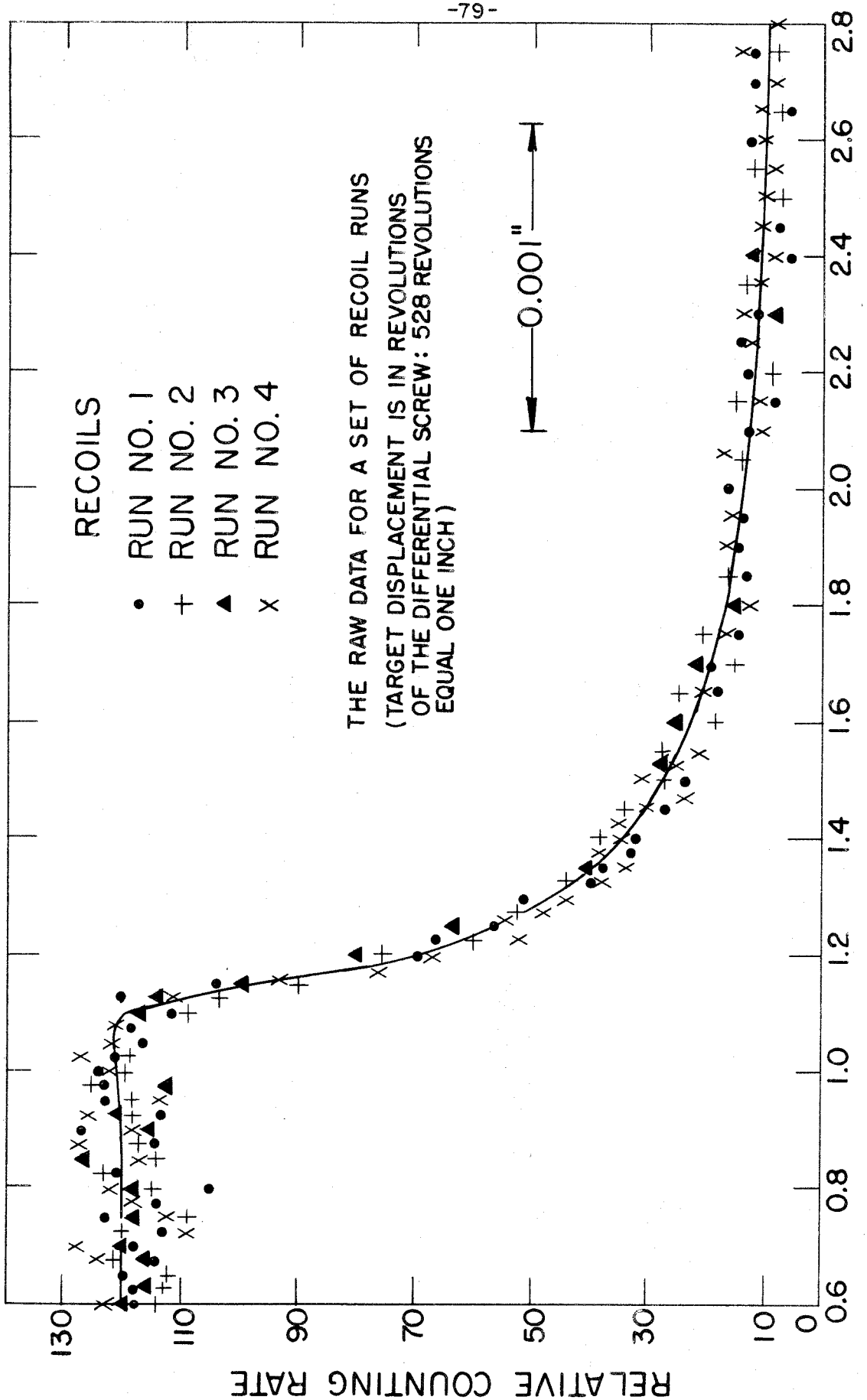
RECOILS
RUN NO. 1
RUN NO. 2
RUN NO. 3
RUN NO. 4
THE RAW DATA FOR A SET OF RECOIL RUNS
(TARGET DISPLACEMENT IS IN REVOLUTIONS
OF THE DIFFERENTIAL SCREW: 528 REVOLUTIONS
EQUAL ONE INCH)
0.001"
RELATIVE COUNTING RATE
TARGET DISPLACEMENT
130
110
90
70
50
30
10
0
0.6
0.8
1.0
1.2
1.4
1.6
1.8
2.0
2.2
2.4
2.6
2.8

FIGURE 18.

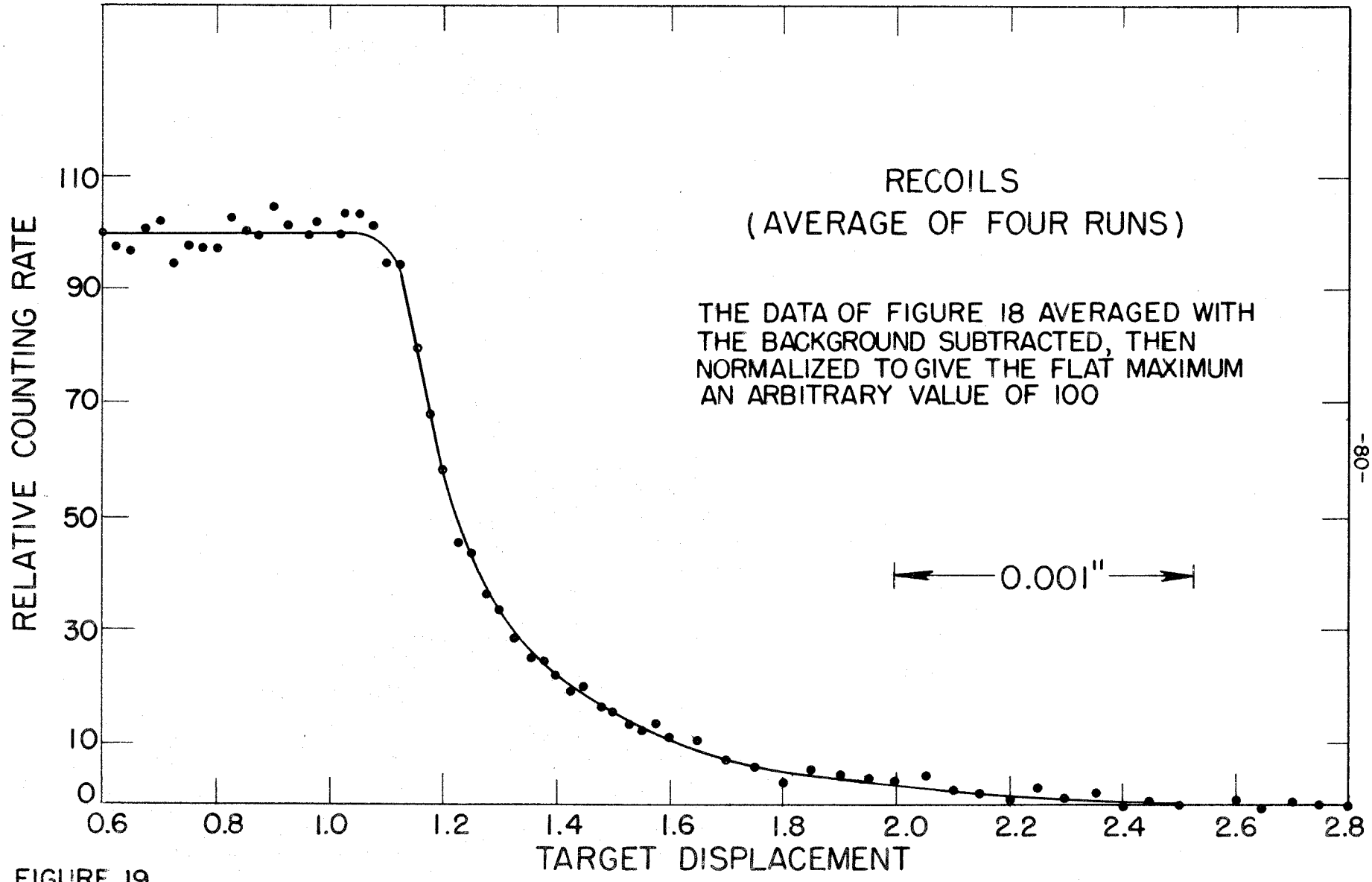
RECOILS
(AVERAGE OF FOUR RUNS)
THE DATA OF FIGURE 18 AVERAGED WITH THE BACKGROUND SUBTRACTED, THEN NORMALIZED TO GIVE THE FLAT MAXIMUM AN ARBITRARY VALUE OF 100
0.001"
RELATIVE COUNTING RATE
110
90
70
50
30
10
0
0.6
0.8
1.0
1.2
1.4
1.6
1.8
2.0
2.2
2.4
2.6
2.8
TARGET DISPLACEMENT

FIGURE 19

SCHEMATIC OF THE GEOMETRY FOR THE ANALYSIS OF THE RECOIL DISTRIBUTION OF DECAYING O^{16} NUCLEI.

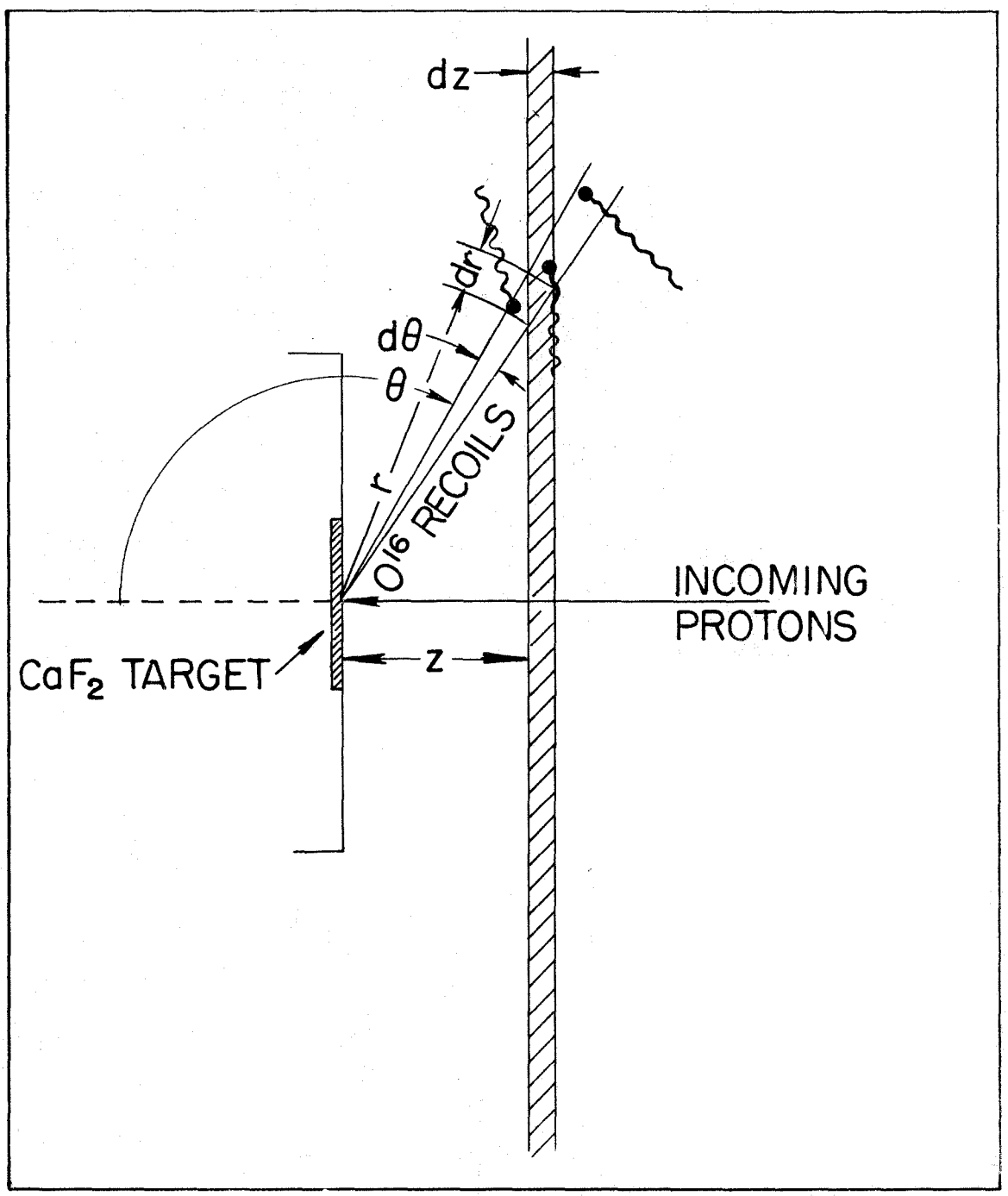

SCHEMATIC FOR DISTRIBUTION OF O^{16} DECAYS

FIGURE 20.

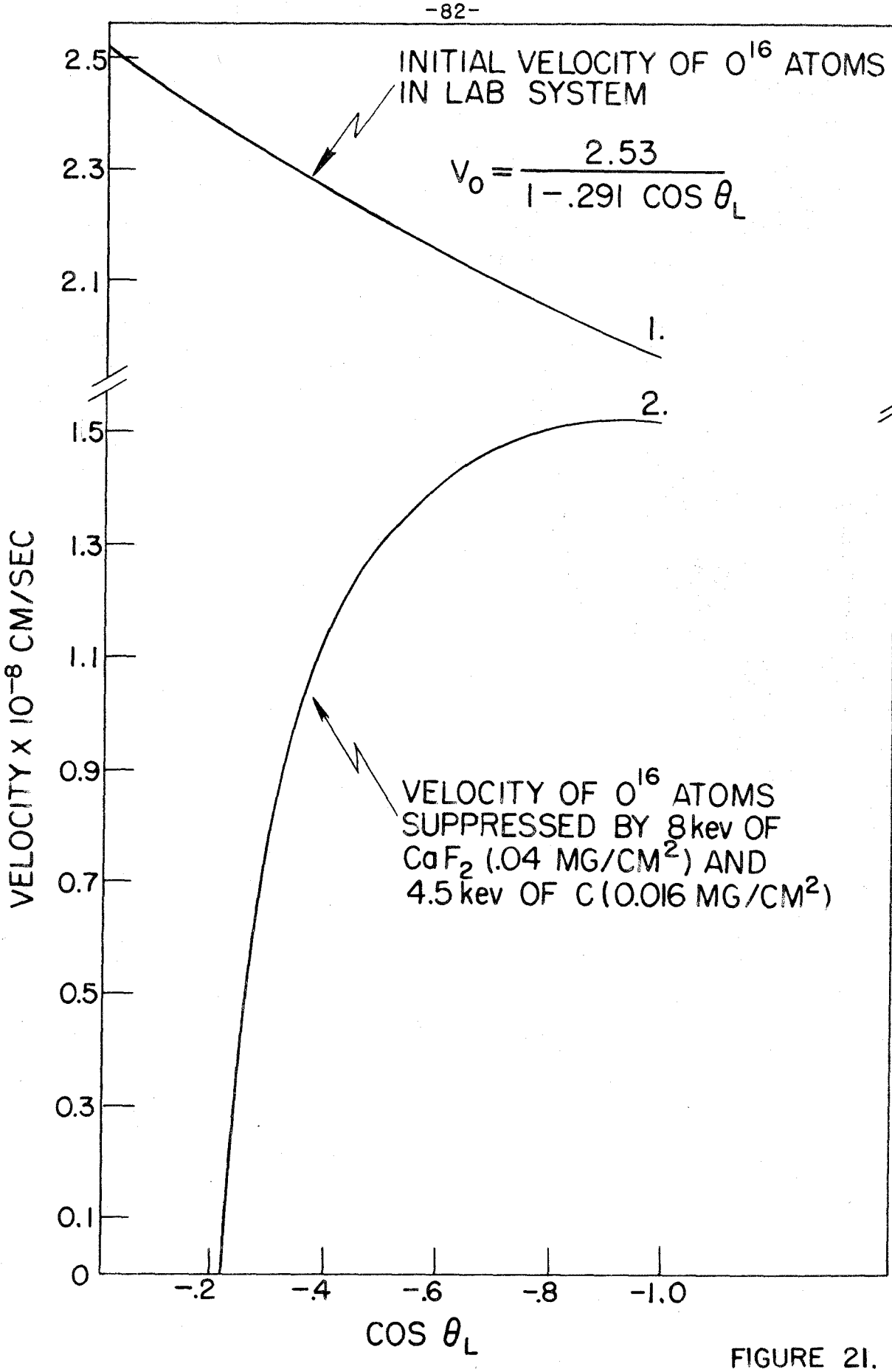
INITIAL VELOCITY OF O^{16} ATOMS IN LAB SYSTEM
$V_0 = \frac{2.53}{1 - .291 \cos\theta_L}$
1.
2.
VELOCITY OF O^{16} ATOMS SUPPRESSED BY 8 kev OF CaF_2 (.04 MG/CM^2) AND 4.5 kev OF C (0.016 MG/CM^2)
VELOCITY X 10^{-8} CM/SEC
2.5
2.3
2.1
1.5
1.3
1.1
0.9
0.7
0.5
0.3
0.1
0
-.2
-.4
-.6
-.8
-1.0
COS θ_L

FIGURE 21.

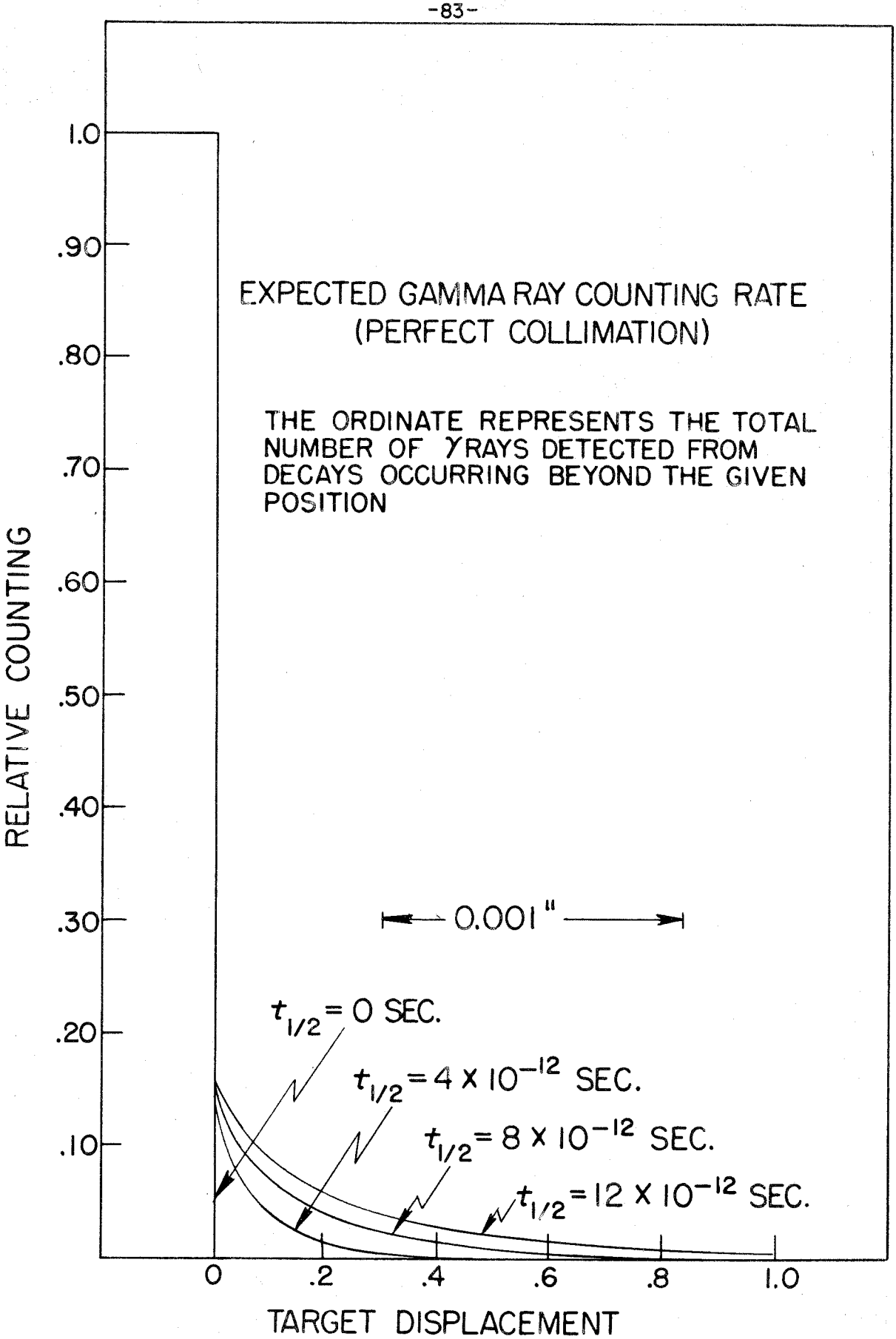
EXPECTED GAMMA RAY COUNTING RATE
(PERFECT COLLIMATION)
THE ORDINATE REPRESENTS THE TOTAL NUMBER OF γ RAYS DETECTED FROM DECAYS OCCURRING BEYOND THE GIVEN POSITION
RELATIVE COUNTING
1.0
.90
.80
.70
.60
.50
.40
.30
.20
.10
0.001"
$t_{1/2}$ = 0 SEC.
$t_{1/2} = 4 \times 10^{-12}$ SEC.
$t_{1/2} = 8 \times 10^{-12}$ SEC.
$t_{1/2} = 12 \times 10^{-12}$ SEC.
0
.2
.4
.6
.8
1.0
TARGET DISPLACEMENT

FIGURE 22.

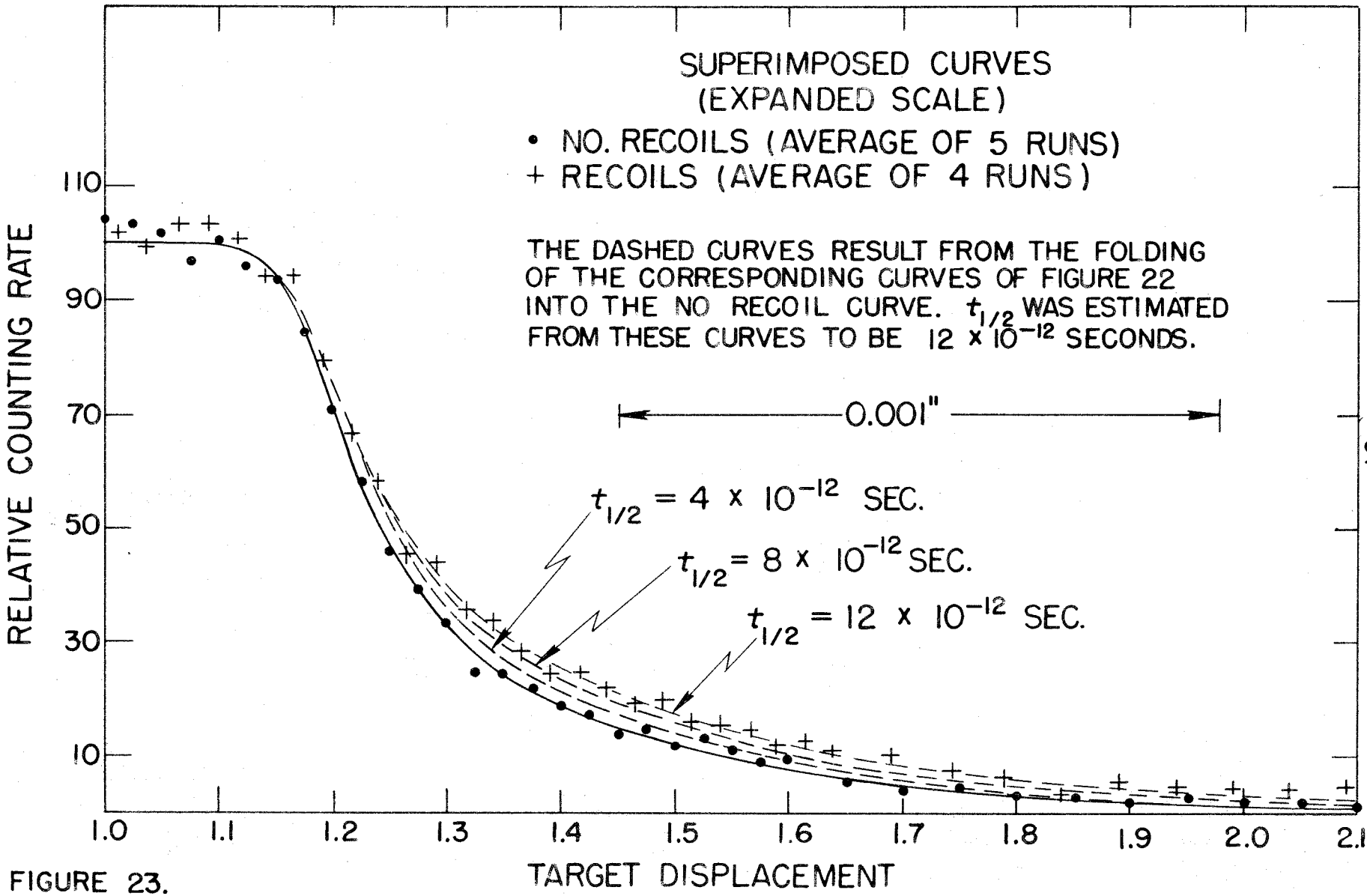
SUPERIMPOSED CURVES
(EXPANDED SCALE)
• NO. RECOILS (AVERAGE OF 5 RUNS)
+ RECOILS (AVERAGE OF 4 RUNS)
THE DASHED CURVES RESULT FROM THE FOLDING OF THE CORRESPONDING CURVES OF FIGURE 22 INTO THE NO RECOIL CURVE. $t_{1/2}$ WAS ESTIMATED FROM THESE CURVES TO BE 12×10^{-12} SECONDS.
0.001"
$t_{1/2} = 4 \times 10^{-12}$ SEC.
$t_{1/2} = 8 \times 10^{-12}$ SEC.
$t_{1/2} = 12 \times 10^{-12}$ SEC.
RELATIVE COUNTING RATE
110
90
70
50
30
10
1.0
1.1
1.2
1.3
1.4
1.5
1.6
1.7
1.8
1.9
2.0
2.1
TARGET DISPLACEMENT

FIGURE 23.

ADDENDUM

On the Sum Rules Involved in the Analysis of Section III. D.

In order to obtain the first sum rule to be considered here, one must first express as a matrix product the expectation value of the absolute square of the appropriate multipole operator for the electric charge distribution (electric octupole in this case) in the ground state of the nucleus of interest. The result is as follows

$$\langle 0|e\sum_{i=1}^{z} r_i^3 Y_3^m(\theta_i,\phi_i)|^2 0\rangle = \sum_n |\langle n|e\sum_{i=1}^{z} r_i^3 Y_3^m(\theta_i,\phi_i)|0\rangle|^2 \qquad \text{A IV (1)}$$

where $e\sum_{i=1}^{z} r_i^3 Y_3^m(\theta_i,\phi_i)$ is the electric octupole operator, and the index, i, ranges over the z protons only. If the approximation is made that the nucleon motion is completely uncorrelated, then the left hand side of this equation can be evaluated since the cross terms in the angular variables will cancel out, giving rise to the expression $\frac{e^2}{4\pi} z\langle 0|r^6|0\rangle$, or equivalently, when $A = 2z$ as for O^{16}, $\frac{e^2}{8\pi}A\langle 0|r^6|0\rangle$, where now, for convenience, the index on r has been dropped and the result of the summation indicated by the factor z. Thus, one arrives at the following form for the sum rule,

$$\sum_n |\langle n|e\sum_{i=1}^{z} r_i^3 Y_3^m(\theta_i,\phi_i)|0\rangle|^2 = \frac{e^2}{8\pi}A\langle 0|r^6|0\rangle \qquad \text{A IV (2)}$$

which gives the sum of the absolute squares of the E3 matrix elements between the ground state and each of the excited states of the system (the left hand side of the equation) in terms of the expectation value of r^6 in the ground state, where r is the radial position of charge in the nucleus. (See also the text of this thesis (page 49) for a somewhat different emphasis on the nature and derivation of this sum rule.)

When one is interested in using this sum rule to fix limits to gamma-ray transition rates between states of zero isotopic spin, as in the case here, where the sum in A IV (2) is to be restricted to excited states of zero isotopic spin, then the right hand member of that equation should be reduced by a factor of two. This can be seen from the following argument. The electric charge operator for the nucleon can be written as $\frac{e}{2}(1+\tau_3)$ and at the same time the sum in the left hand side of A IV (1) extended to all A nucleons. However, only the isoscalar part, $\frac{e}{2}$, of the charge operator can contribute to a zero to zero isotopic spin transition, and hence, when the E3 operator is squared and summed over all A nucleons, it gives for the required expectation value $(\frac{1}{2})^2 \frac{A}{z}$ $(= \frac{1}{2}$ when $A = 2z)$ times the corresponding result obtained when all excited states are counted. This restricted sum rule, then, is the one used to obtain the lifetime limit given in the text. (See page 49 for the further assumptions involved in that calculation.)

Another sum rule which is very useful for such a problem as this is one involving the evaluation of $\langle 0|r^4|0\rangle$ rather than the $\langle 0|r^6|0\rangle$ required in the above sum rule. The derivation given below follows that given by Ferrell (33) for an electric monopole sum rule.

First, consider a function B, of the form $B = \sum_i g_i$ where g_i is a function of the spatial coordinates of the ith nucleon alone, and evaluate the double commutator, $[B,[H, B]]$, where H is the Hamiltonian of the nuclear system. This results in

$$[B,[H, B]] = 2BHB - BBH - HBB. \qquad \text{A IV (3)}$$

Now, take the expectation value of these quantities in the ground state of the system, and remembering that H is diagonal when the representation

used is the set of eigenstates of H, one obtains the following

$$\langle 0|[B,[H,B]]|0\rangle = \sum_n (2B_{on}H_{nn}B_{no} - B_{on}B_{no}H_{oo} - H_{oo}B_{on}B_{no}) =$$

$$\sum_n 2|\langle n|B|0\rangle|^2(H_{nn} - H_{oo}) = \sum_n 2|\langle n|B|0\rangle|^2 \hbar\omega_{no}. \qquad \text{A IV (4)}$$

Using for H the form, $\frac{1}{2}\sum_{\substack{ij \\ i\neq j}} V_{ij} - \sum_i \frac{h^2}{2M}\nabla_i^2$, the left hand member of A IV (4) may be readily evaluated to give $\frac{\hbar^2}{M}\langle 0|\sum_i|\nabla_i g_i|^2|0\rangle$, where we confine ourselves to T = 0 to T = 0 transitions so that we need only the isotopic spin independent part of B which will commute even with the exchange part of V_{ij}; otherwise a correction for exchange forces is necessary. No assumptions as to the internal nucleon-nucleon correlations have been made. If now, the functions, g_i, are specified to be the E3 multipole charge distribution operators and the sum is carried out over the z protons, then the following sum rule results

$$\sum_n |\langle n|e\sum_{i=1}^{z} r_i^3 Y_3^m(\theta_i,\phi_i)|0\rangle|^2 \hbar\omega_{no} = \frac{21\hbar^2 z}{8\pi M}\langle 0|r^4|0\rangle \qquad \text{A IV (5)}$$

$$= \frac{21\hbar^2 A}{16\pi M}\langle 0|r^4|0\rangle \text{ (when } A = 2z).$$

Following the same argument as presented above, the right hand member of this equation should be decreased by a factor of two (assuming A = 2z) when considering zero to zero isotopic spin gamma-ray transitions. Again, the remaining details of the calculation of the lifetime limit, obtained with this sum rule for the 6.14-Mev transition in O^{16}, are discussed in the text.

It is perhaps of some interest to note that the first sum rule, as reduced to the form given in equation A IV (2), gives directly the sums

of squares of the matrix elements of the E3 operator, but requires the assumption of no nucleon-nucleon correlations. The second sum rule, however, requires no such assumption as to correlations, but involves instead, the introduction of the energy difference corresponding to each E3 transition matrix element. Thus, on one hand, the use, in practice, of the first sum rule is limited by the lack of knowledge of the internal nucleon-nucleon correlations in the ground state. On the other hand, the use of the second sum rule is similarly limited, but the limitation now appears instead in the form of the lack of knowledge of the energy spectrum of the states of the system.

A further discussion of various sum rules and their uses has been given by Blatt and Weisskopf (34) and, in addition, Sachs and Austern (35) have presented an interesting discussion of sum rules for electric multipole radiation.